OPTIMUM VIBRATION CONTROL OF FLEXIBLE BEAMS BY PIEZO-ELECTRIC ACTUATORS

BY

A.BAZ and S.POH

MECHANICAL ENGINEERING DEPARTMENT
THE CATHOLIC UNIVERSITY OF AMERICA
WASHINGTON, D.C. 20064

NASA CONTRACT #30429-D

MARCH 1987

ACKNOWLEDGEMENTS

Special thanks are due to the Space Science and Technology branch at NASA Goddard Space Flight Center for providing the funds necessary to conduct this study under contract No.30429-D.

Thanks are particularly due to Mr. Phil Studer for his invaluable inputs and for his engineering insight that have been instrumental in the initiation and implementation of this effort.

Special thanks are also due to Dr. Joseph Fedor and Mr. Eric Osborne for their interest in the Independent Modal Space Control Method and for their continuous thought stimulating discussions and invaluable suggestions that have contributed considerably to this study.

ABSTRACT

This study deals with the utilization of piezo-electric actuators in controlling the structural vibrations of flexible beams.

A Modified Independent Modal Space Control (MIMSC) method is devised to enable the selection of the optimal location, control gains and excitation voltage of the piezo-electric actuators in a way that would minimize the amplitudes of vibrations of beams to which these actuators are bonded, as well as the input control energy necessary to suppress these vibrations.

The developed method accounts for the effects that the piezo-electric actuators have on changing the elastic and inertial properties of the flexible beams.

Numerical examples are presented to illustrate the application of the developed MIMSC method in minimizing the structural vibrations of beams of different materials when subjected to different loading and end conditions using ceramic or polymeric piezo-electric actuators.

The obtained results emphasize the importance of the devised method in designing more realistic active control systems for flexible beams, in particular, and large flexible structures in general.

NOMENCLATURE

b	width of beam and piezo-actuator, m
B_{ii}	partitioned matrices of the modal shape matrix, i=C or R
d	electric charge constant of piezo-actuator, m/v
D	distance to neutral axis of composite beam measured from its lower edge, m
$E_{1,2}$	Young's modulus of elasticity of piezo-actuator and beam respectively, N/m^2
E_i	Young's modulus of elasticity of element i of the beam, N/m^2
f	vector of modal forces and moments, N or Nm
F	vector of external forces and moments, N or Nm
f_C	modal forces acting on the controlled modes, N or Nm
F_C	physical forces applied to control C modes, N or Nm
f_i	modal force controlling the i^{th} mode, N or Nm
F_i	vector of external forces and moments acting on element i , N or Nm.
f_R	modal forces acting on the residual modes, N or Nm
F_r	physical forces acting on the residual modes, N or Nm
$g_{1,2}$	modal position and velocity feedback gains
$I_{1,2}$	area moment of inertia of actuator and beam about the neutral axis of the composite beam respectively, m^4
I_i	area moment of inertia of the element i, m^4
J_i	mass moment of inertial of the composite beam at node i, $kg\text{-}m^2$
K_i	stiffness matrix of the element i
K	overall stiffness matrix of beam-actuator system

L_i length of element i, m

m_i mass of the composite beam at node i, kg

M mass matrix of beam-actuator system

M_{ei} external moment acting on i^{th} node of beam, Nm

M_f piezo-electric moment generated by piezo-film, Nm

N number of elements of the beam

R weighting factor

$t_{1,2}$ thickness of piezo-actuator and beam respectively, m

u_i modal displacement of node i, m

$\dot{u}_i$ modal velocity of node i, m

U modal coordinates of the flexible system

v voltage applied across the piezo-electric film, volts

V_i external force acting on the i^{th} element of the beam, N

y_i the linear translation of node i, m

$w_{b,f}$ beam and film mass per unit length respectively, kg/m

Greek Letters

γ_i factor=1 or zero if actuator is bonded to element i or not respectively

δ_i deflection of node i, m or rad.

δ deflection vector of all nodes of the beam, m or rad.

$\ddot{\delta}$ acceleration vector of all nodes of the beam, m/s^2 or rad/s^2

ϵ_f piezo-electric strain in piezo-actuator, m/m

θ_i angular deflection of node i, rad.

λ diagonal matrix of the eigenvalues of the system

$\sigma_{1,2}$ bending stresses in piezo-actuator and beam

respectively N/m^2

σ_f piezo-electric stress in actuator, N/m^2

ϕ modal shape matrix of the eigenvectors of the flexible system

ω_i resonant frequency at the i^{th} normal mode, rad./s

Superscripts

T designates transpose

-1 designates inverse

INTRODUCTION

Active vibration control systems are becoming essential and viable means for minimizing the vibrations of large flexible structures which are intended to provide stable bases for precision pointing in space. Such control systems aim at compensating for the inherently low natural damping characteristics of the flexible structures in order to suppress their oscillatory behavior over a wide band of excitation frequencies without compromising their structural integrity. In this way, it would be possible to meet the strict operational and functional constraints which are currently imposed on these structures.

Distinct among the presently available active control systems are those that rely in their operation on piezo-electric actuators. Such systems have proven to be experimentally effective in controlling the vibrations of simple structural elements such as rectangular beams [1-2]* and hollow cylindrical masts [3]. The effectiveness of these systems is coupled also with the light weight, high force and low power consumption capabilities of the piezo-electric actuators [4-8]. These features rendered this class of actuators to be an attractive candidate for controlling structural vibrations.

---

* Numbers between brackets designate references at end of report

The present state-of-the-art of this type of actuators has been limited to the analysis and testing of their characteristics [9-11] as influenced by their geometrical or operational conditions. A recent attempt has been made by Baz [12], to select their optimal geometrical parameters and location which are best suited for a particular structure subjected to known static loading conditions. The developed synthesis procedure has proven to be essential to the successful integration of the actuators into the structure in order to minimize its static deformation.

However, no effort has been done to optimize the control of the vibrations of a multi-mode flexible system using a small number of optimally placed piezo-actuators through the development of efficient and realistic control algorithm that ensures minimal amplitudes of oscillation and input control energy.

It is, therefore, the purpose of this study to devise such an optimal control method that is based on a modification of the well known Independent Modal Space Control(IMSC) method [13-15]. The devised method accounts for the spillover from the controlled modes into the uncontrolled modes due to the use of fewer actuators than the modeled modes. The developed method incorporates also an optimal placement procedure that will enable the selection of the optimal location of the piezo-electric actuators in the structure in order to guarantee a balance between the

suppression of the amplitudes of vibration and the input control energy.

Furthermore, the developed procedure considers the effect that the piezo-electric actuators have on changing the elastic and inertial properties of the structure to which they are bonded to. Such changes result in modifying the normal modes of the structure one way or another depending on the location of the actuator.

In this study, the emphasis will be placed on piezo-electric actuator-beam systems to illustrate the devised control strategy. But, without any further modifications, the developed method can be readily applied to large structures.

THE PIEZO-ELECTRIC ACTUATOR-BEAM SYSTEM

A. General Layout

Figure (1) shows a general layout of a flexible beam A whose vibration is to be controlled by piezo-electric actuator B. The beam, under consideration, can generally be made of several steps which are not necessarily of the same thickness or the same material. The interfacial nodes between the different steps can be subjected to external forces, moments or both. Further, the degrees of freedom of any node can be limited to linear translations, angular rotations or restrained completely depending on the nature of support at the node under consideration.

In this study, the beam is assumed to have rectangular cross section of constant width b. The beam is considered to deflect in the transverse direction due to the flextural action of the external forces and moments.

In Figure (1), the piezo-electric actuator B is shown bonded to the element i of the flexible beam to form a composite beam. When an electric field is applied across the film, then it will expand if the field is, for example, along the polarization axis of the film and will contract if the two were out of phase. The expansion or contraction of the film relative to the beam, by virtue of the piezo-electric effect, creates longitudinal bending stresses in the

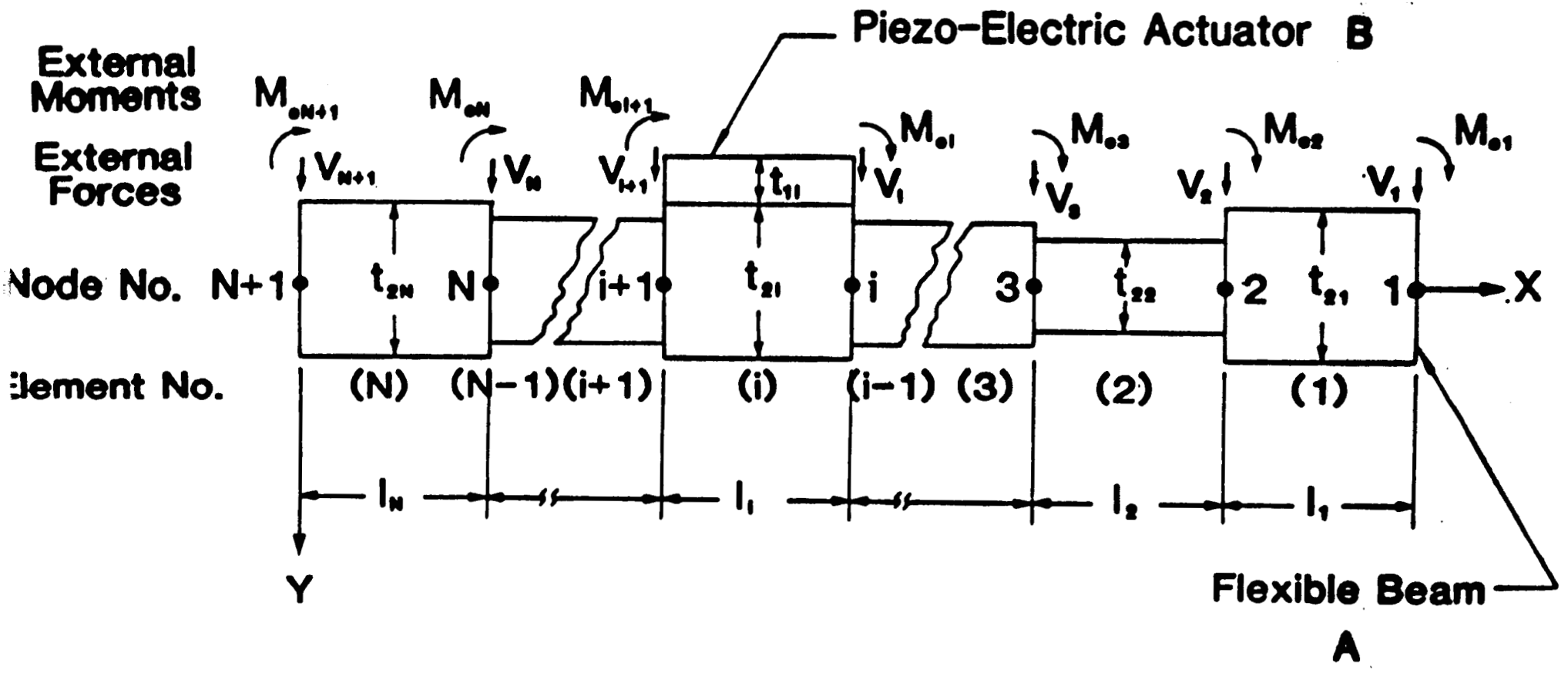

Figure (1) – General layout of the piezo-electric actuator–beam system

composite beam which tend to bend the beam in a manner very similar to a bimetallic thermostat.

With proper selection, placement and control of the actuator, it would be possible to generate enough piezo-electric bending stresses to counter balance the effect of the exciting forces and moments acting on the beam in a way that minimizes its structural vibrations.

B. Finite Element Model Of An Actuator-Beam Element

Figure (2) shows a schematic drawing of a piezo-film A bonded to an element B of the flexible beam.

If a voltage v is applied across the film, a piezo-electric strain ϵ_f is introduced in the film and can be computed from :

$$\epsilon_f = (d/t_1)*v \qquad (1)$$

where d is the electric charge constant of the film, m/v

t_1 is the thickness of the piezo-electric actuator, m

This strain results in a longitudinal stress σ_f given by :

$$\sigma_f = E_1(d/t_1)*v \qquad (2)$$

where E_1 is the Young's modulus of elasticity of the film,

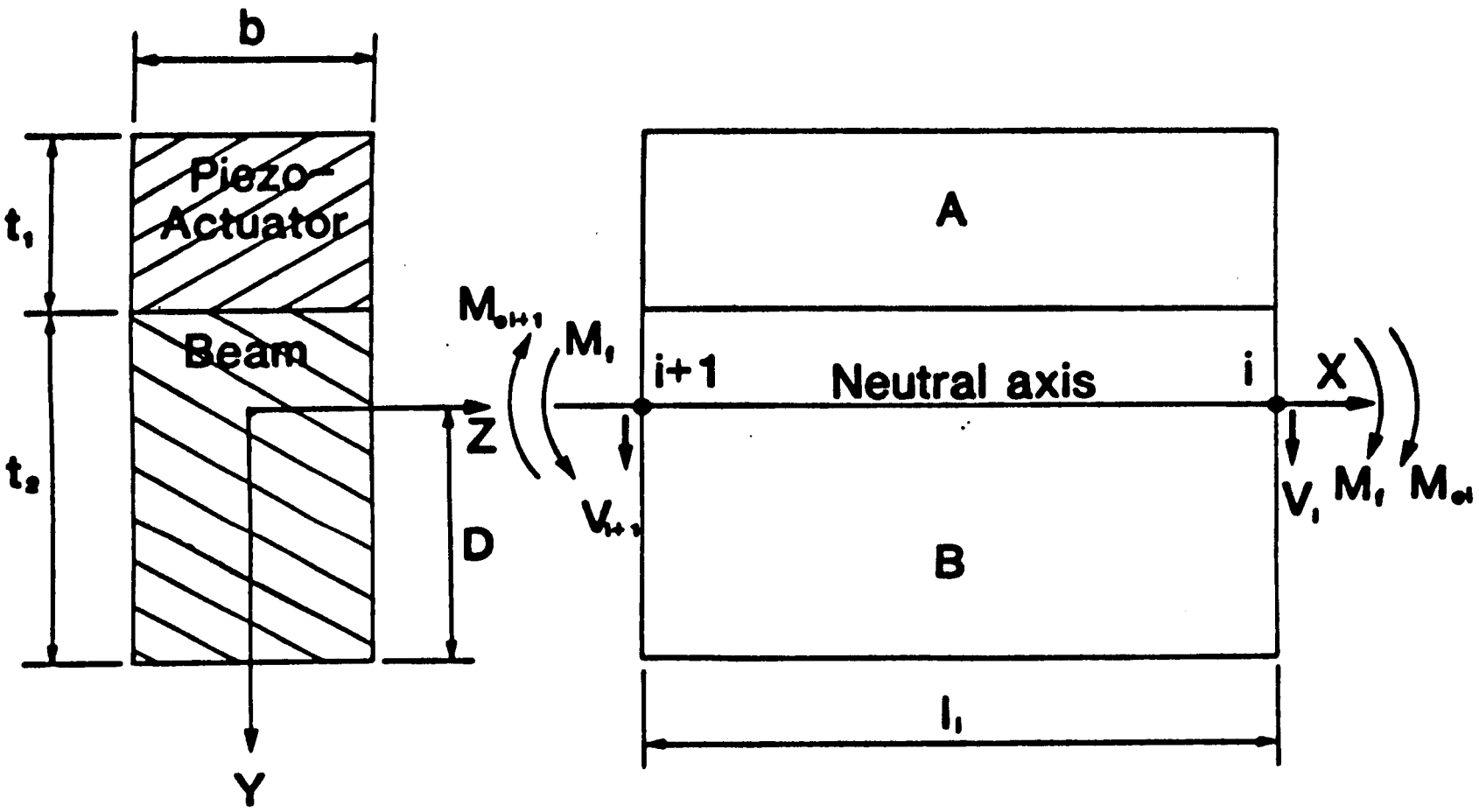

Figure (2) – Schematic drawing of an actuator bonded to a flexible beam element

N/m^2

This, in turn generates a bending moment M_f, around the neutral axis of the composite beam, given by :

$$M_f = \int_{-(t_2-D)}^{-(t_1+t_2-D)} \sigma_f (b*y) dy \qquad (3)$$

where t_2 is the thickness of the beam, m

b is the width of the beam and the piezo-film, m

In equation (3), D is the distance of the neutral axis from the lower edge of the beam which can be determined by considering the force balance in the longitudinal direction X of the beam, or :

$$\int_{\text{film}} \sigma_1 dA + \int_{\text{beam}} \sigma_2 dA = 0 \qquad (4)$$

or

$$E_1 b \int_{-(t_1+t_2-D)}^{-(t_2-D)} y dy + E_2 b \int_{-(h_2-D)}^{D} y dy = 0 \qquad (5)$$

where E_2 is Young's modulus of elasticity of the beam, N/m^2

Equation (5) yields the following expression for D :

$$D = \frac{E_1 t_1^2 + 2E_1 t_1 t_2 + E_2 t_2^2}{2(E_1 t_1 + E_2 t_2)} \tag{6}$$

Equation (2), (3) and (6) can be combined to determine the bending moment M_f generated by the piezo-film on the composite beam as follows :

$$M_f = \frac{d*b*(t_1+t_2)*(E_1 E_2 t_2)*v}{2*(E_1 t_1 + E_2 t_2)} \tag{7}$$

For this composite beam, it can be easily shown [16] that it has a flextural rigidity ($E_i I_i$) given by :

$$E_i I_i = E_1 I_1 + E_2 I_2 \tag{8}$$

where I_1 and I_2 are the area moments of inertia of the film and the beam about the neutral axis respectively.

Let us now assume that the composite beam, shown in Figure (2), extends a length l_i between two nodes (i) and (i+1). Further, it is assumed that the external forces V_i and V_{i+1} as well as the external moments M_{ei} and M_{ei+1} are acting on the beam at nodes i and i+1 respectively. Then, the resulting linear and angular deformations of the beam y_i and θ_i as well as y_{i+1} and θ_{i+1} at the nodes i and i+1, respectively, can be related to the loads acting on the element as follows [17] :

$$\begin{bmatrix} V_i \\ M_{ei}+M_f \\ V_{i+1} \\ M_{ei+1}-M_f \end{bmatrix} = \frac{E_i I_i}{L_i^3} \begin{bmatrix} 12 & 6L_i & -12 & 6L_i & y_i \\ 6L_i & 4L_i^2 & -6L_i & 2L_i^2 & \theta_i \\ -12 & -6L_i & 12 & -6L_i & y_{i+1} \\ 6L_i & 2L_i^2 & -6L_i & 4L_i^2 & \theta_{i+1} \end{bmatrix} \quad (9)$$

Equation (9) can be rewritten as :

$$F_i = K_i \delta_i \quad (10)$$

where F_i is the resultant forces and moments vector acting on the beam element i, N

K_i is the stiffness matrix of the composite beam element i, N/m

δ_i is the deflection vector of the nodes bounding the beam element, m

Equation (9) constitutes the basic finite element model that relates the external loads (V and M_e) and piezo-electric moments (M_f) to the deflections (y and θ) of the element as a function of its elastic and inertial parameters.

The equation can be equally used for any element of the beam whether it has a piezo-film bonded to it or not. In the latter case, M_f is set to zero and flextural rigidity $E_i I_i$ is set equal to that of the flexible beam element under consideration.

The force-displacement characteristics of the individual elements of the beam-actuator system, as given for element i by equation (9), are combined to determine the overall stiffness of the beam system.

The equilibrium conditions of the overall structure will be expressed as :

$$\begin{matrix}\text{External forces and moment}\\ \text{acting on the nodes}\\ \text{of the overall system}\end{matrix} = \sum \begin{matrix}\text{forces and moments}\\ \text{acting on the elements}\\ \text{at these nodes}\end{matrix}$$

or

$$F = \sum_{i=1}^{N+1} F_i = \sum_{i=1}^{N+1} K_i \delta_i = K\delta \qquad (11)$$

where K is the overall stiffnessmatrix of the system (2n*2n)

Bathe and Wilson [18], Yang [19] and Fenner [20], for example, show how to generate the overall matrix K from the stiffness matrices K_i of the individual elements.

The inertial properties of the composite actuator-beam system are determined using the lumped mass method where the mass and rotational inertial of each element is distributed among the nodes bounding the element [17].

Therefore, the diagonal mass matrix M (2n*2n) for the actuator-beam system, shown in Figure(1), can be written as :

$$M = \begin{bmatrix}
m_1 & 0 & \cdots & & & & & & & & 0 \\
0 & J_1 & 0 & \cdots & & & & & & & \vdots \\
0 & 0 & m_2 & 0 & \cdots & & & & & & \vdots \\
\vdots & \vdots & 0 & J_2 & 0 & \cdots & & & & & \vdots \\
\vdots & \vdots & \ddots & \ddots & \ddots & \ddots & & & & & \vdots \\
\vdots & \vdots & & & 0 & m_i & 0 & \cdots & & & \vdots \\
\vdots & \vdots & & & & 0 & J_i & 0 & \cdots & & \vdots \\
\vdots & \vdots & & & & & 0 & m_{i+1} & 0 & \cdots & \vdots \\
0 & \cdots & & & & & & 0 & J_{i+1} & 0 \cdots & \vdots \\
\vdots & \vdots & & & & & & & \ddots & \ddots & \vdots \\
\vdots & \vdots & & & & & & & & 0 \; m_N \; 0 & \vdots \\
\vdots & \vdots & & & & & & & & 0 \; J_N \; 0 & \vdots \\
\vdots & \vdots & & & & & & & & 0 \; m_{N+1} & 0 \\
0 & 0 & \cdots & & & & 0 & \cdots & & 0 & J_{N+1}
\end{bmatrix} \qquad (12)$$

where $m_1 = [(w_b+\gamma_1 w_f)*L_1]/2$

$J_1 = [(w_b+\gamma_1 w_f)*L_1^3]/2$

$m_i = [(w_b+\gamma_{i-1} w_f)*L_{i-1}+(w_b+\gamma_i w_f)*L_i]/2$

$J_i = [(w_b+\gamma_{i-1} w_f)*L_{i-1}^3+(w_b+\gamma_i w_f)*L_i^3]/12$

$m_{N+1} = [(w_b+\gamma_N w_f)*L_N]/2$

$J_{N+1} = [(w_b+\gamma_N w_f)*L_N^3]/12$

$w_{b,f}$ = beam and film mass per unit length respectively, kg/m.

γ_i = 1 if an actuator is bonded to beam element i. 0 if not.

The stiffness and mass matrices K and M, defined by equations 11 and 12, are used to define the dynamic equations of motion of the actuator-beam system.

The equations of motion of the actuator-beam system can be written as follows :

$$M\ddot{\delta} + K\delta = F \tag{13}$$

where $\ddot{\delta}$ is the acceleration of the nodal points of the composite beam, m/s^2

Equation (13) is put in the self-adjoint modal space by using the following weighted modal transformation [21] :

$$\delta = \phi U \tag{14}$$

where U is the modal coordinates of the system

ϕ is the weighted modal shape matrix of the eigenvectors of the flexible system

Using such transformation, reduces the coupled equation of motion (13) to the following uncoupled form :

$$\ddot{U} + \lambda U = f \tag{15}$$

where λ is a diagonal matrix of the eigenvalues of the system

f is the modal force matrix given by

$$f = \phi^T F \tag{16}$$

The modal representation of the flexible beam-actuators system is utilized, as a basis for this study, as it makes the design and the selection of the gains of the active control systems rather simple as compared to the coupled system representation. This is due to the fact that the design of modal controllers using, for example, the Independent Modal Space Control (IMSC) method [13-15] has been proven, in numerous studies such as [15], to be computationally more efficient than the conventional Riccati or Pole Assignment methods.

CONTROL STRATEGY OF ACTUATOR-BEAM SYSTEM

The control strategy used in controlling the vibration of the flexible beam system is based on a modified version (MIMSC) of the Independent Modal Space Control (IMSC) method. Details of the method are presented in Reference [22]. In essence, the MIMSC utilies small number of optimally placed actuators to control a large system that has large number of degrees of freedom. The method accounts also for the effect of interaction between the controlled and uncontrolled modes.

Considering the modal representation of the elastic system, one could rewrite the modal forces f as :

$$[f] = \begin{bmatrix} f_C \\ f_R \end{bmatrix} = \begin{bmatrix} \phi_1(l_1)....\phi_1(l_C) & \phi_1(l_{C+1})....\phi_1(l_N) \\ \cdots\cdots\cdots\cdots\cdots\cdots\cdots\cdots \\ \phi_C(l_1)....\phi_C(l_C) & \phi_C(l_{C+1})....\phi_C(l_N) \\ \phi_{C+1}(l_1)..\phi_{C+1}(l_C) & \phi_{C+1}(l_{C+1})..\phi_{C+1}(l_N) \\ \cdots\cdots\cdots\cdots\cdots\cdots\cdots\cdots \\ \phi_N(l_1)....\phi_N(l_C) & \phi_N(l_{C+1})... \phi_N(l_N) \end{bmatrix} * \begin{bmatrix} F_C \\ F_R \end{bmatrix} \qquad (17)$$

where $f_{C,R}$ are the modal forces on the controlled and residual modes respectively.

$F_{C,R}$ are the physical forces on the controlled and residual modes.

$\phi_i(l_j)$ is the modal shape at mode i and location l_j.

The above equation can be rewritten as :

$$\begin{bmatrix} f_C \\ f_R \end{bmatrix} = \left[\begin{array}{c|c} B_{CC} & B_{CR} \\ \hline B_{RC} & B_{RR} \end{array}\right] * \begin{bmatrix} F_C \\ F_R \end{bmatrix} \qquad (18)$$

If only C modes are controlled with equal number of control forces F_C, then F_R=0 and equation (18) reduces to :

$$f_C = B_{CC}F_C \qquad (19)$$

and

$$F_R = B_{RC}F_C \qquad (20)$$

In the IMSC method, it is assumed that the control forces F_C will not contribute to the excitation of the residual higher order modes. Accordingly, it was assumed that f_R=0. This of course can only be true if the number of controlled modes is very large compared to the number of residual modes or when the residual modes are at much higher frequency band than the controlled modes. If these two conditions are not satisfied, then there will be considerable interaction between the controlled and residual modes.

The MIMSC method considers such interaction by calculating the optimal modal control forces $[f_C]$ using the IMSC close form solution of the Riccati Equation such that the control force f_i of the i^{th} mode, as given by [14], is :

$$f_i = -(g_1 \omega_i u_i + g_2 \dot{u}_i)/R \tag{21}$$

where R is a factor that weighs the importance of minimizing the vibration with respect to the control forces.

ω_i is the resonant frequency at the i^{th} normal mode.

u_i, $\dot{u}_i$ are the modal displacement and velocity respectively.

g_1, g_2 are the modal position and velocity feedback gains given by [22] as :

$$g_1 = -\omega_i R + \sqrt{(\omega_i R)^2 + \omega_i{}^2 R} \tag{22}$$

$$g_2 = \sqrt{2R\omega_i[-\omega_i R + \sqrt{(\omega_i R)^2 + \omega_i{}^2 R}] + \omega_i{}^2 R} \qquad (23)$$

Accordingly, the displacement u_i and velocity $\dot{u}_i$ at the i^{th} mode can be feedback and used along with equations (21), (22) and (23) to determine the modal control force f_i.

Once these forces are calculated, equation (19) is solved to give the physically applied control forces F_C as follows :

$$F_C = B_{CC}{}^{-1} \bullet f_C \qquad (24)$$

Then equation (20) is used to calculate the modal forces f_R that would excite the residual modes and which are generated by the spillover from the controlled modes. Definitely these f_R are not equal to zero as originally assumed in the IMSC method.

Equations (17) and (15) can then be integrated with respect to the time to determine the modal displacements (u_i) and velocities ($\dot{u}_i$) which can, in turn, be used again to compute the modal forces f and so on.

From the modal displacements and velocities, the physical state (δ) of the flexible system can be determined from equation (14). A relationship can therefore be established between the physical state δ of the system and the physical control forces F_C applied to it.

It is very important to point out here that the magnitude of the modal forces f_C depends primarily on the magnitude ω_i's of the controlled modes as well as the modal state variables u and $\dot{u}$. On the other hand, the magnitude of the actual physical control forces F_C depends mainly, for a given controlled mode, on the point of application of these forces as defined by the matrix B_{CC}^{-1}. Therefore, minimizing f_C does not necessarily means that F_C will be minimum inspite of the fact that it is represented as a linear combination of f_C. This is simply because the coefficients of the linear combination, which are elements of the B_{CC}^{-1} matrix, depend on the placement strategy of the control forces F_C. One could still find an optimally placed set of physical control forces F_C such that the physical displacements and control forces would assume minimum value.

This optimum placement of the physical control forces is an important feature of the MIMSC method and will be demonstrated to be essential part of the design of the active control system.

One should stress here also that if all the modes are controlled and there is no residual modes then the conditions for minimizing f_C will make F_C minimum as well. But, in real large structures this will be unlikely to happen as the number of controlled modes is much smaller than the number of modeled modes. Therefore, it is essential to augment the IMSC

method with an optimal placement algorithm to guarantee efficient design of the control system.

The optimum placement of the actuators is implemented through the use of the Univariate Search method [23] which varies the location of one actuator at a time in order to :

$$\text{Minimize} \int (\ddot{q}^2 + RF_c^2)\, dt \qquad (25)$$

In other words, the optimal placement algorithm minimizes the weighted sum of the amplitudes of vibration and the generated control forces. The weighting factor R is selected by the designer to emphasize the importance of damping out the vibration over the expended control energy (when $R<<1$) or vice versa when $R>>1$. Equal importance of the two parameters is achieved with $R=1$.

The MIMSC method incorporates also an extremely important feature which is based on the "TIME SHARING" of a small number of actuators in the modal space to control large number of modes. Details of such important feature are presented in References [29-30]. In few words, the Time Sharing Control Strategy generates modal control forces to control, at the first time interval, the first through the C^{th} modes using C actuators then, at the second time interval, it provides signals to control the second through the $(C+1)^{th}$ modes followed by commands to control the third through the $(C+2)^{th}$ modes and so on until all the modeled

modes are controlled in this sequential fashion. Once all the modeled modes have received their share from the control action the cycle is repeated again to effectively damp out all the modes of vibration with few number of actuators. This strategy has been shown to result in efficient control of the vibration of large structures with relatively small number of actuators when other existing methods fail to do so [22].

Figure (3) outlines a flowchart of the MIMSC method indicating the main steps of optimal placement and time sharing of the actuators as well as the consideration of the spillover between the controlled and residual modes.

Application Of MIMSC Method To Piezo Actuators-Beam System

The MIMSC method is utilized to design active vibration controllers for flexible beams of particular configuration when subjected to specific external loading and end conditions. The controllers rely in their operation on one or more piezo-electric actuators which are optimally selected, placed and controlled without violating their polarization or strength constraints. Two types of piezo-electric actuators are considered in this study namely : ceramics and polymeric actuators whose physical properties are given in Table (1).

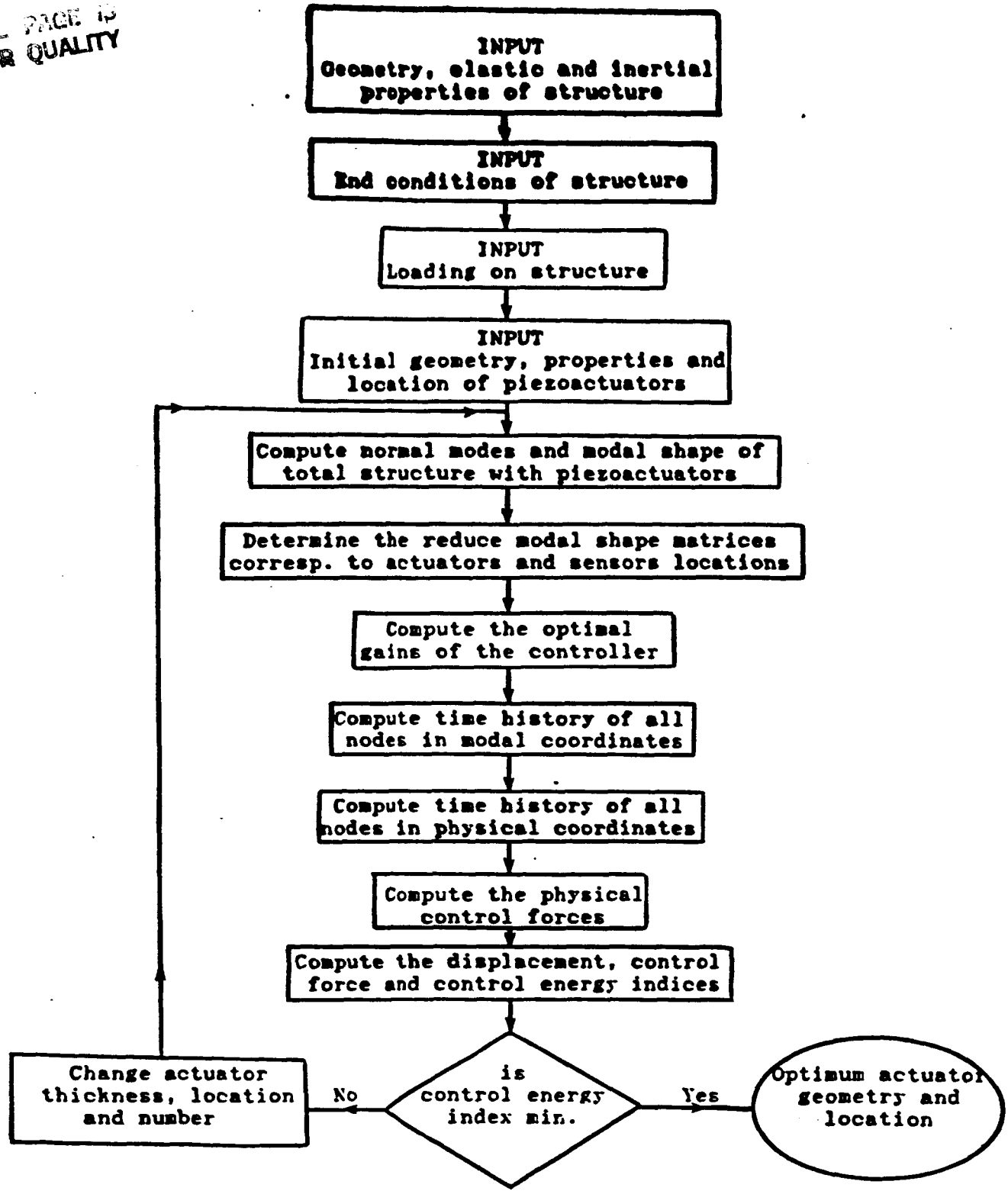

Figure (3) - Flow chart of the MIMSC Computational Algorithm

Table (1) - Properties of piezo-electric actuators

Actuator Type	Ceramic(Ref.8&10)		Polymeric(Ref.24)
Material	PZT	G1278	KYNAR (PVF2)
Charge coefficient d 10^{-12} (m/v)	123	270	23
Young's modulus (G N/m^2)	139	60	2
Max. voltage v (Mv/m)	1	0.7	30
Max. tensile strength ($M N/m^2$)	45	47.5	33 - 55
Density (kg/m^3)	7500	7400	1780

NUMERICAL EXAMPLES

The application of the MIMSC method is illustrated by considering a flexible straight beam, shown in Figure (4), which is 0.0125m wide, 0.0021m thick and 0.15m long. The beam is modeled by three-element model for the sake of demonstrating the MIMSC method.

The effect of varying beam loading and end conditions as well as beam and actuator materials on the optimal configuration of the system is considered in great details.

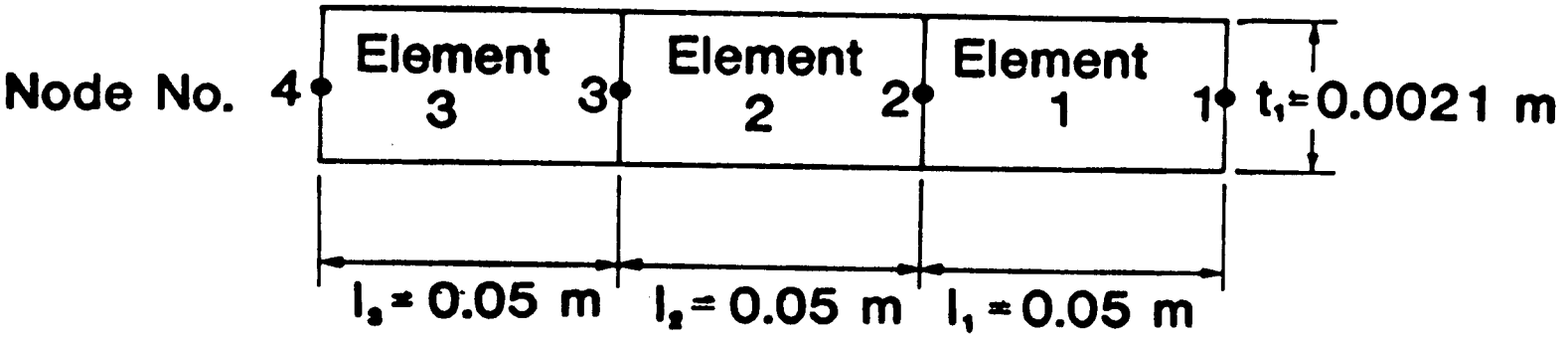

Figure (4) – Layout of a 3–element straight beam

A. Vibration of Cantilever Beam

The flexible beam, under consideration, is restrained at node 1 to form a cantilever beam whose free end, node 4, is subjected to either transverse impulsive loading or sinusoidal excitations. The considered impulsive load is selected to have a magnitude of 0.1N and duration of 1.0ms whereas the sinusoidal excitations are assumed to have the same magnitude of 0.1N and a frequency ranging between 15 to 1000 Hz.

The effect of the two types of loading on the time and/or the frequency responses of the piezo electric controlled beam is determined using the MIMSC method and compared to the corresponding characteristies of the uncontrolled beam. Such comparison are used to determine the effectiveness of piezo-electric actuators in damping out the vibrations of the undamped flexible beam.

(I). Response to The Impulsive Loading

Figures (5-a) and (5-b) show the time histories of the amplitudes of transverse vibrations of the uncontrolled beam when it is made of steel and aluminum respectively. It can be seen that the beams will continue to vibrate in a limit cycle fashion even after termination of the input impulse. This is due to the fact that the beams are assumed to have no inherent structural damping.

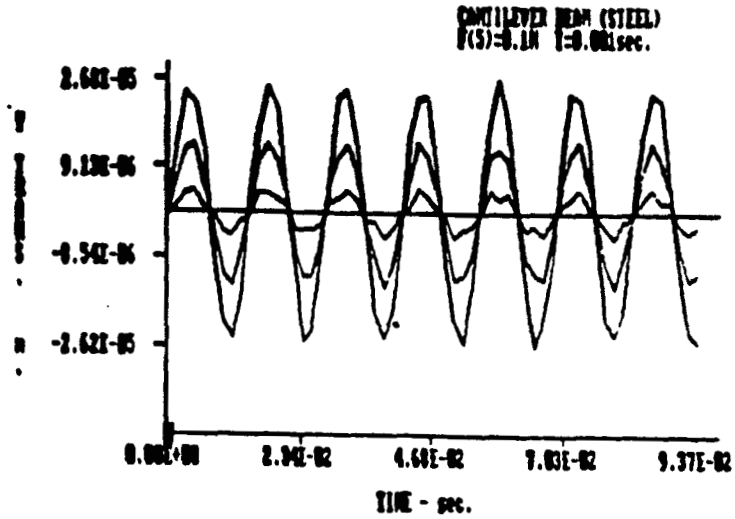

Figure (5-a) - Time history of the amplitudes of transverse vibration of uncontrolled steel cantilever beam when subjected to transverse impulsive loading.

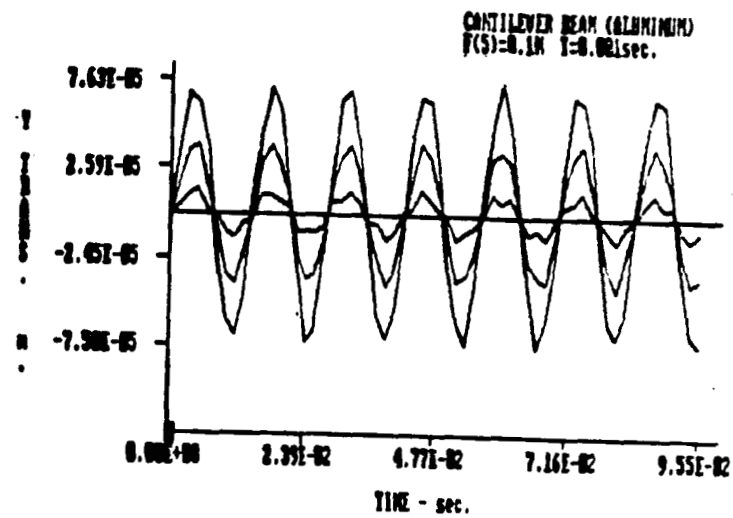

Figure (5-b) - Time history of the amplitudes of transverse vibration of uncontrolled aluminum cantilever beam when subjected to transverse impulsive loading.

The figures indicate also that the aluminum beam will experience higher amplitudes of vibrations than the steel beam.

The amplitudes of vibrations displayed in Figures (5-a) and (5-b) are used as a datum for measuring the effect of the thickness, material, location and number of piezo-electric actuators on controlling the vibration of the cantilever beam as will be described in that follows.

(a). Effect of Actuator Thickness

Figures (6-a), (6-b) and (6-c) illustrate the time histories of the amplitudes of transverse vibrations of the steel cantilever beam when controlled by the MIMSC method using one piezo-electric actuator that has a thickness of 0.000525m, 0.00105m and 0.0021m respectively. In dimensionless form, the actuators are selected to have thicknesses equal to 1/4, 1/2 and 1 that of the beam thickness respectively. All the considered actuators are made of PZT4 ceramic are placed between nodes 1 and 2, i.e. bonded to the element near the fixed end of the beam.

Figures (7-a), (7-b) and (7-c) display the corresponding control voltages generated, according to the MIMSC method, to power the considered four actuators respectively.

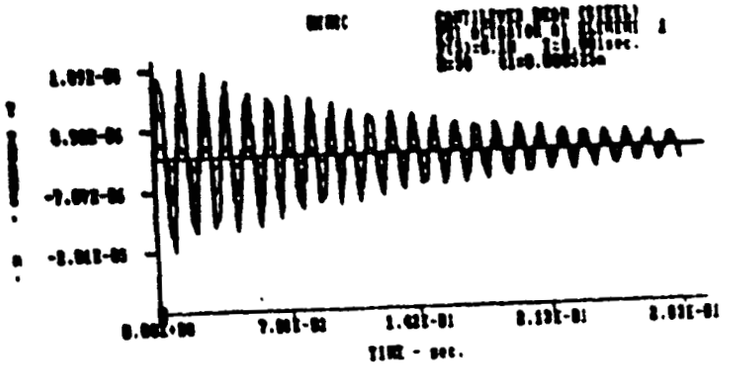

Figure (6-a) - Time history of the amplitudes of transverse vibration of a steel cantilever beam controlled by one PZT actuator of a thickness=0.000525 m placed at element 1.

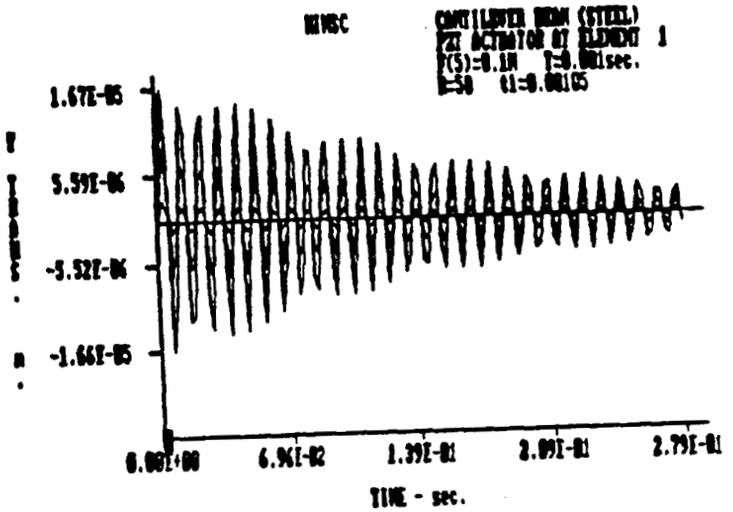

Figure (6-b) - Time history of the amplitudes of transverse vibration of a steel cantilever beam controlled by one PZT actuator of a thickness=0.00105 m placed at element 1.

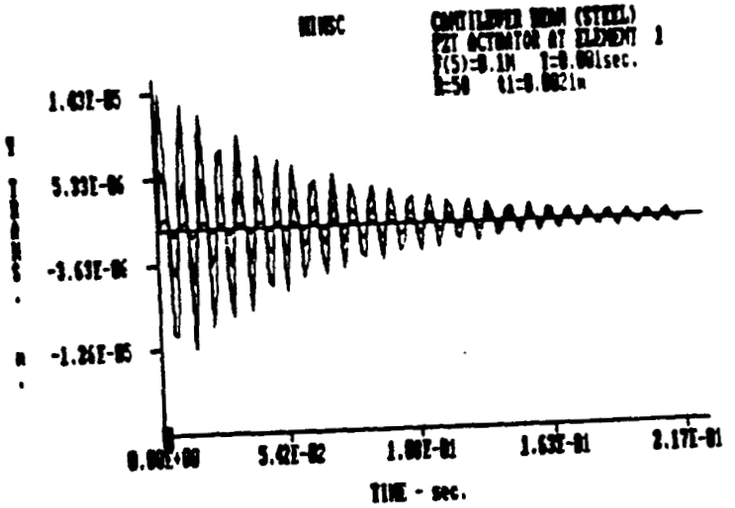

Figure (6-c) - Time history of the amplitudes of transverse vibration of a steel cantilever beam controlled by one PZT actuator of a thickness=0.0021 m placed at element 1.

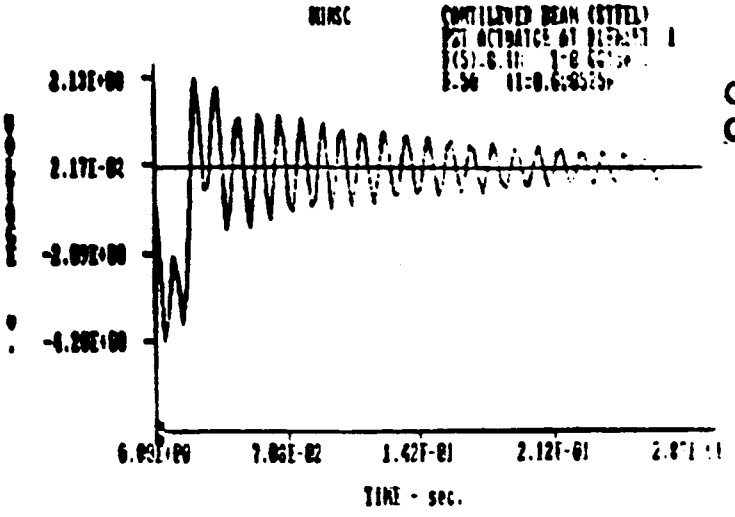

Figure (7-a) - Time history of the control voltages required to control a steel cantilever beam by one PZT actuator of a thickness =0.000525 m placed at element 1.

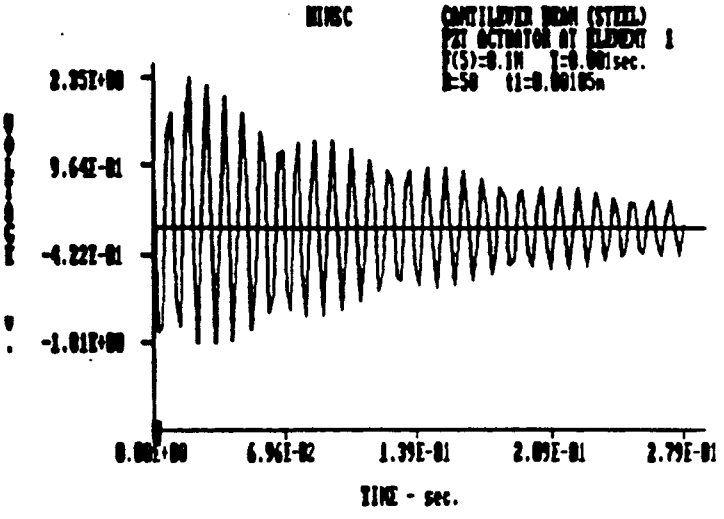

Figure (7-b) - Time history of the control voltages required to control a steel cantilever beam by one PZT actuator of a thickness=0.00105 m placed at element 1.

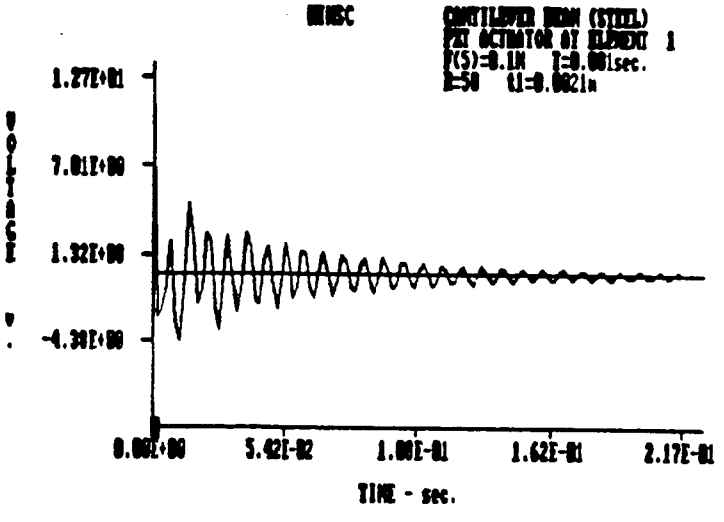

Figure (7-c) - Time history of the control voltages required to control a steel cantilever beam by one PZT actuator of a thickness =0.0021 m placed at element 1.

Figures (6-a) through (6-c) indicate that using one actuator which is capable only of producing bending moments, it was possible to control all the three linear translations and the three angular rotations of the cantilever beam. This feature is an important feature of the MIMSC method where one actuator is shared to control more than one mode of vibration of the flexible structure.

Detailed analysis of the figures is summarized in Table (2) to indicate the effect of the thinkness of the piezo-electric actuator on the displacement index U_d, control force index U_c and control energy index U_E. These indices are defined by the following expressions:

$$U_d = \sum_{t=0}^{t=t^{\bullet}} \sum_{i=1}^{N} \delta_i^{\,2} * \Delta t \qquad (26)$$

$$U_c = \sum_{t=0}^{t=t^{*}} \sum_{i=1}^{N} F_i^{\,2} * \Delta t \qquad (27)$$

$$U_E = \sum_{t=0}^{t=t^{\bullet}} \sum_{i=1}^{N} |\dot{\delta}_i * F_i| \, \Delta t \qquad (28)$$

where Δt is time increment for integrating the equations of motion taken as :

$$\Delta t = 1/10*2*3.1416/\omega_{max} \qquad (29)$$

ω_{max} maximum natural mode of vibration of the elastic

system, rad/sec

t^* maximum time of integration, sec

N number of degrees of freedom of the structure

Table (2) - Effect of actuator thickness on the displacement, control force and control energy indices for a steel cantilever beam controlled with one PZT actuator at element 1

Thickness (mm)	0.525	1.050	2.100	4.200	8.400
Displacement Index, $x10^9$	2.264	1.750	1.354	1.195	0.975
Control force Index, $x10^9$	4.740	5.299	6.003	10.337	3616.300
Control Energy Index, $x10^6$	0.354	0.343	0.350	0.307	28.690

Table (2) indicates clearly that increasing the thickness of the actuator results in decreasing the amplitude of vibrations of the beam considerably as measured by the displacement index U_d. Such a reduction is attributed primarily to the stiffness effect that result from bonding thicker actuators to the original flexible beam. However, using such thicker actuators would require large control forces to damp out the vibrations of the beam-actuator system. This is reflected directly into high control voltages as can be seen clearly from Figures (7-a) through (7-c).

Therefore, we have a push and a pull situation where thicker actuators are preferred to minimize the amplitudes of oscillation and thinner actuators are desirable if one is to limit the magnitude of the control forces and control voltages. Accordingly, a balance can be achieved between

minimizing the displacement index without having to produce excessively large control forces. This balance can be attained, if we consider the control energy index U_E which is a measure of the energy spent to control the vibration of the beam. From Table (2), it can be seen that there is an optimum actuator thickness, t=4.2mm, at which the control energy index assumes a minimum value.

One should also point out here that using the piezoactuators results in damping out completely the vibrations of the beam when compared to the case of the uncontrolled beam as can be seen from a comparison between Figures (6-a), (6-b), (6-c) and (5-a) respectively.

It is important to note here that bonding the different thickness actuators to the beam is found to result in changing the natural modes of vibration of the beam significantly. For example, with an actuator thickness equals to 1/4 the beam thickness the first normal mode occurs at 67Hz but when the thickness is increased to the beam thickness, the first mode decreased to 55.3Hz. Therefore, It is essential to consider the effect of introducing the actuators on changing the elastic and inertial properties of the flexible system before designing the active control system.

Also, it is essential to note that the design of the active modal controller is carried out with a weighting

factor R=50 in order to maintain the control forces low enough to avoid depolarization but high enough to control effectively the beam system. Detailed account for the effect of the weighting factor R on the dynamics of the beam system will be given later on.

(b) Effect of Number of Actuators

The effect of the actuator thickness should also be considered in view of the number of actuators to be used in controlling the vibration of the steel beam. For example, considering the case of two actuators to be used to control the six degrees of freedom of the beam. The considered two actuators are made of PZT of the same thickness and placed at elements 1 and 3. The effect of varying the thickness of the two actuators from 1/4 to 4 times the beam thickness on the vibration of the beam is shown in Figures (8-a) through (8-c) respectively. The corresponding control voltages are displayed in Figures (9-a) through (9-c).

Figures (8-a), (8-b) and (8-c) indicate that increasing the thickness of the actuators produced favorable damping characteristics as it results in reducing the maximum amplitude of transverse vibration of the beam. But this is on the expense of a significant increase in the required control voltages. For example, increasing the actuator thickness from 1/4 to 4 times the beam thickness reduces the maximum amplitude of vibration from 2.05E-5m to 1.06E-5m whereas it

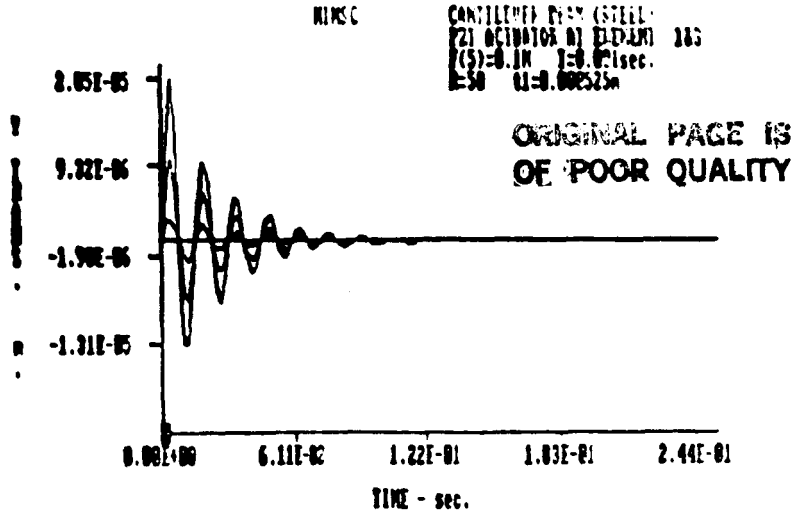

Figure (8-a) - Time history of the amplitudes of transverse vibration of a steel cantilever beam controlled by two PZT actuators of a thickness=0.000525 m placed at elements 1 and 3.

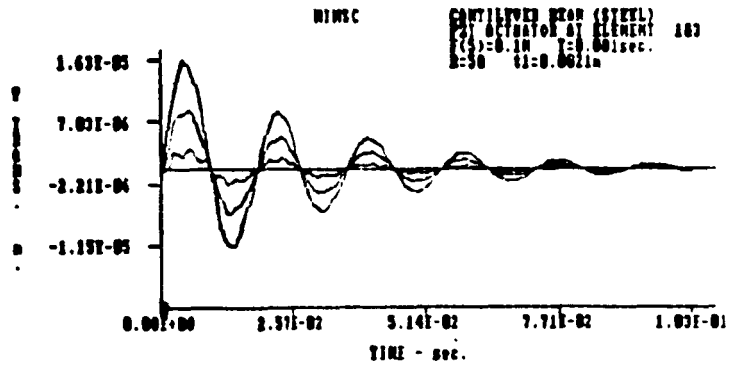

Figure (8-b) - Time history of the amplitudes of transverse vibration of a steel cantilever beam controlled by two PZT actuators of a thickness=0.0021 m placed at elements 1 and 3.

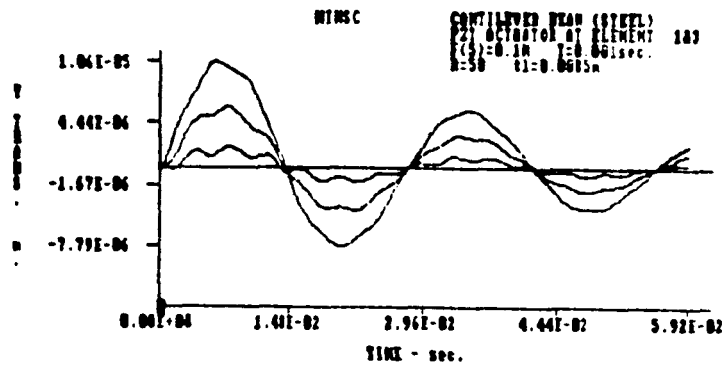

Figure (8-c) - Time history of the amplitudes of transverse vibration of a steel cantilever beam controlled by two PZT actuators of a thickness=0.0085 m placed at elements 1 and 3.

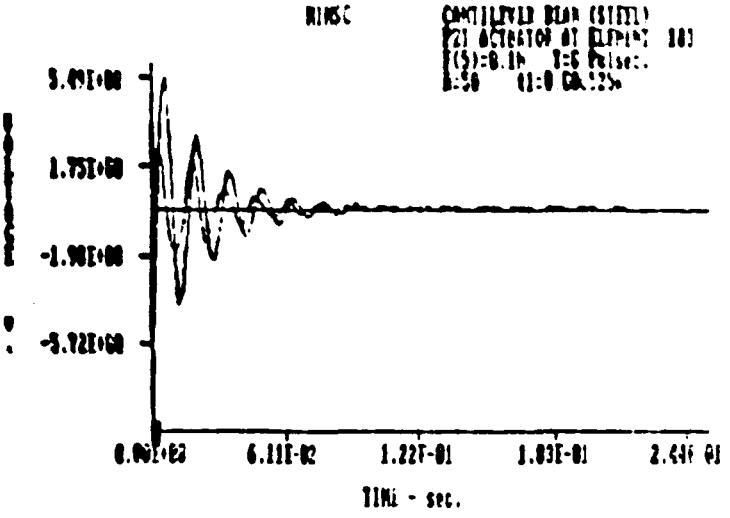

Figure (9-a) - Time history of the control voltages required to control a steel cantilever beam by two PZT actuators of a thickness=0.000525 m placed at elements 1 and 3.

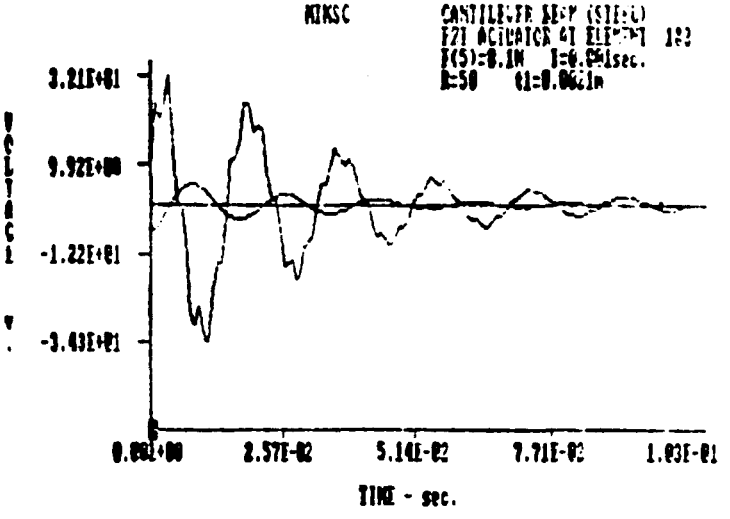

Figure (9-b) - Time history of the control voltages required to control a steel cantilever beam by two PZT actuators of a thickness=0.0021 m placed at elements 1 and 3.

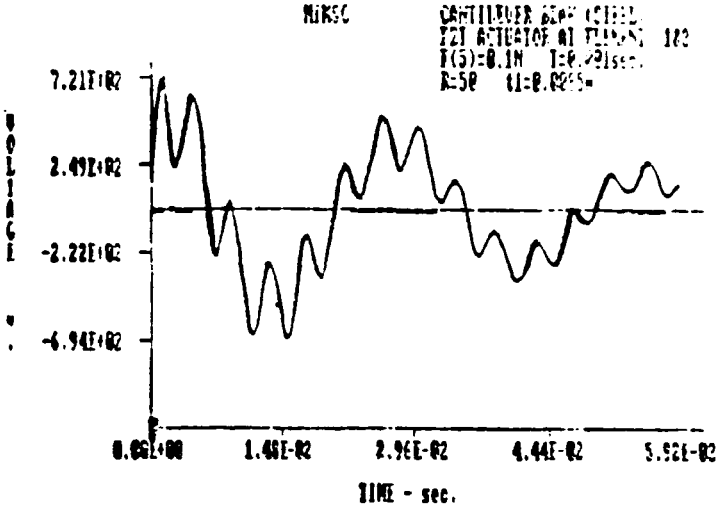

Figure (9-c) - Time history of the control voltages required to control a steel cantilever beam by two PZT actuators of a thickness=0.0084 m placed at elements 1 and 3.

increases the maximum control voltage from 5.5v to 720v. Therefore, the benefits gained by the reduction in the amplitude of vibration are by far less than the drawbacks resulting from excessive control voltages. A proper balance between these two parameters is essential for an optimally controlled system. Such a balance can be attained by considering the control energy index U_E listed in Table (3).

Table (3) - Effect of actuator thickness on the displacement, control force and control energy indices for a steel cantilever beam controlled with two PZT actuators at elements 1 and 3

Thickness (mm)	0.525	2.100	4.200	8.400
Displacement Index, $x10^9$	0.628	0.498	0.412	0.326
Control force Index, $x10^9$	12.140	10.000	33.250	5346.800
Control Energy Index, $x10^6$	0.675	0.515	1.409	70.900

Table(3) suggests that using two actuators each of a thickness equal to that of the original beam results in minimal control energy expenditure.

Furthermore, comparing the results listed in Tables(2)and(3) one could see that it is more beneficial, from the displacement and control energy indices, to use the two optimal actuators to control the beam vibration rather than using just one optimal actuator. This is inspite of the fact the total weight of the two optimal actuators is equal to the optimal single actuator.

Therefore, for a given weight of the structure and the piezoactuators, it is advantageous to distribute the piezo-material over the structural element to minimize its vibrations.

(c) Effect of Actuator Location

(i) Single Actuator

Figures (10-a), (10-b) and (10-c) show the time history of the amplitude of transverse vibration of the steel beam when a PZT piezo-electric actuator, of a thickness twice the beam thickness, is placed at element 1, 2 or 3 respectively. The corresponding control voltages are shown in Figures (11-a), (11-b) and (11-c) for the considered three placement strategies respectively.

The associated displacement, control force and control energy indices are listed in Table (4).

Table (4) - Effect of actuator location on the displacement, control force and control energy indices for a steel cantilever beam controlled with one PZT actuator of thickness=4.2mm

Actuator Location	Element 1	Element 2	Element 3
Displacement Index, $x10^9$	1.195	1.516	1.326
Control force Index, $x10^9$	10.337	356.75	2658.800
Control Energy Index, $x10^6$	0.307	11.07	61.800

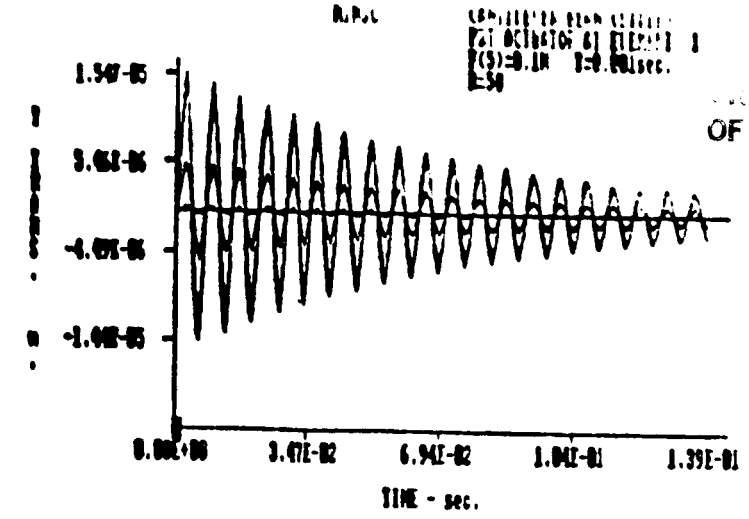

Figure (10-a) - Time history of the amplitudes of transverse vibration of a steel cantilever beam controlled by one PZT actuator of thickness=0.0042 m placed at element 1.

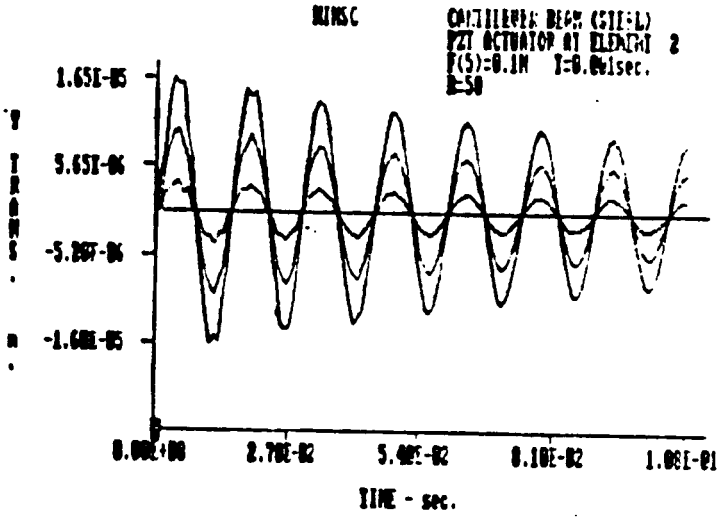

Figure (10-b) - Time history of the amplitudes of transverse vibration of a steel cantilever beam controlled by one PZT actuator of thickness=0.0042 m placed at element 2.

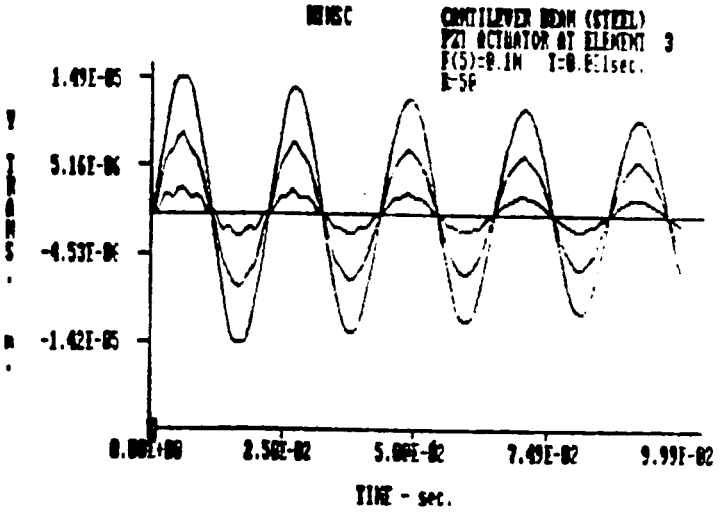

Figure (10-c) - Time history of the amplitudes of transverse vibration of a steel cantilever beam controlled by one PZT actuator of thickness=0.0042 m placed at element 3.

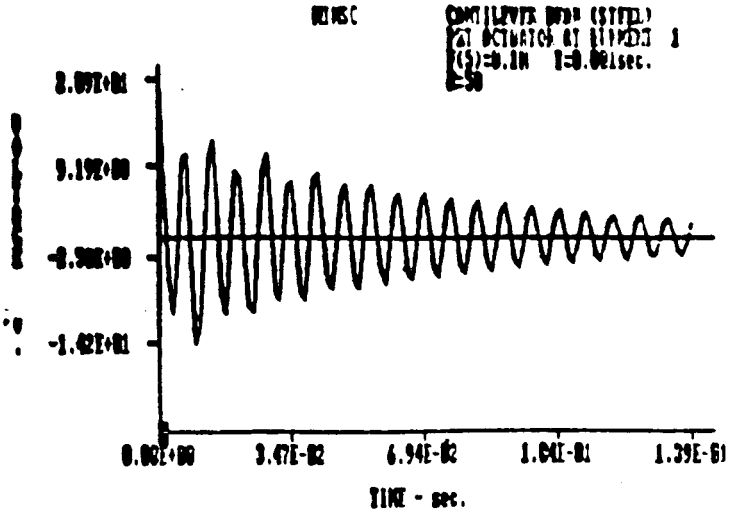

Figure (11-a) - Time history of the control voltages required to control a steel cantilever beam by one PZT actuator of thickness=0.0042 m placed at element 1.

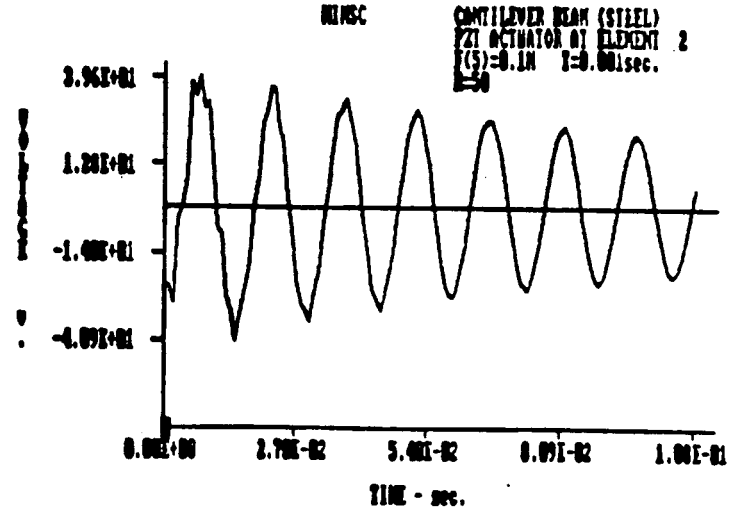

Figure (11-b) - Time history of the control voltages required to control a steel cantilever beam by one PZT actuator of thickness=0.0042 m placed at element 2.

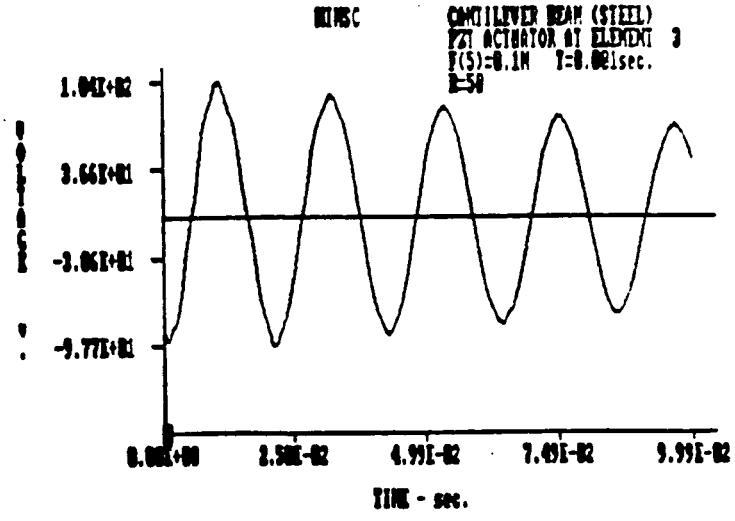

Figure (11-c) - Time history of the control voltages required to control a steel cantilever beam by one PZT actuator of thickness=0.0042 m placed at element 3.

It is, therefore, obvious that when a single actuator is to be used to control the vibrations of the cantilever beam, than this actuator should be bonded to element 1 near the fixed end of the beam. Such a placement strategy is optimal, from all points of views, as it minimizes the displacement, control force and control energy indices all at the same time.

(ii) Two Actuators

When two PZT actuators are used to control the steel cantilever beam, the displacement, control force and control energy indices are as listed in Table (5).

Table (5) - Effect of actuator location on the displacement, control force and control energy indices for a steel cantilever beam controlled with two PZT actuators of thickness=4.2mm

Actuator Location	Element 1 and 2	Element 1 and 3	Element 2 and 3
Displacement Index, $x10^9$	0.342	0.412	0.393
Control force Index, $x10^9$	27.170	33.250	678.360
Control Energy Index, $x10^6$	2.100	1.691	31.170

The obtained results indicated that it is preferable to place the actuators at element 1 and 3 in order to obtain the minimum displacement, control force and control energy indices.

(d) Effect of Weighting Factor R

(i) Single Actuator

Figures (12-a), (12-b) and (12-c) show the time history of the amplitude of transverse vibration of the steel cantilever beam, controlled by one PZT actuator placed at element 1, for values of the weighting factor R of 1, 20 and 35 respectively. The associated time histories of the control voltages are shown in Figures (13-a), (13-b) and (13-c) respectively. A summary of the displacement, control force and control energy indices is given is Table 6 for values of the weighting factor between 1 and 200.

Table (6) - Effect of the weighting factor R on the displacement, control force and control energy indices for a steel cantilever beam controlled with one PZT actuator of thickness=4.2mm placed at element 1

Weighting Factor R	1	20	35	50	100	200
Displacement Index, $x10^9$	0.204	0.778	1.017	1.195	158.26	199.20
Control force Index, $x10^9$	2450	25.200	14.100	10.300	6.18	4.027
Control Energy Index, $x10^6$	9.017	0.497	0.386	0.308	0.227	0.173

The presented figures and the obtained results indicate that emphasizing the importance of the control force over the amplitude of vibration by increasing the value of the weighting factor R results in lowering the magnitude of the

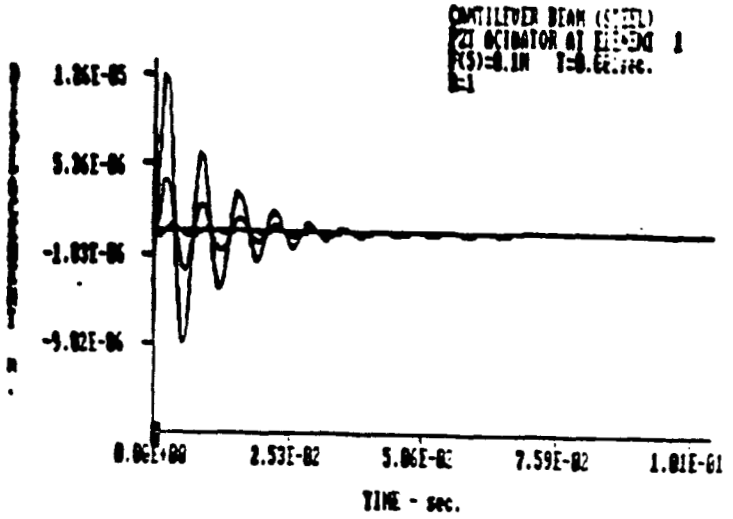

Figure (12-a) - Time history of the amplitudes of transverse vibration of a steel cantilever beam controlled by one PZT actuator placed at element 1 when the weighting factor R=1.

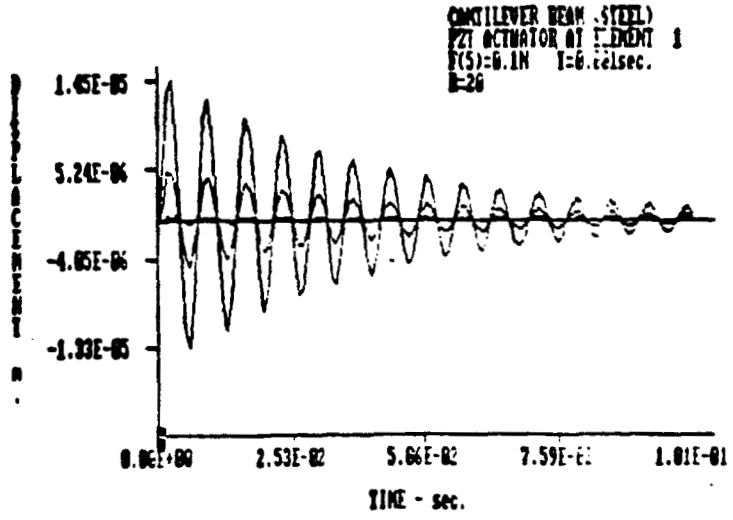

Figure (12-b) - Time history of the amplitudes of transverse vibration of a steel cantilever beam controlled by one PZT actuator placed at element 1 when the weighting factor R=20.

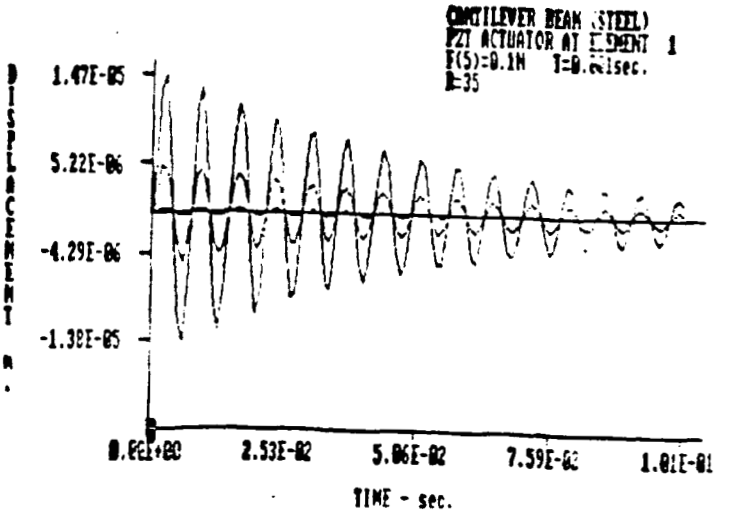

Figure (12-c) - Time history of the amplitudes of transverse vibration of a steel cantilever beam controlled by one PZT actuator placed at element 1 when the weighting factor R=35.

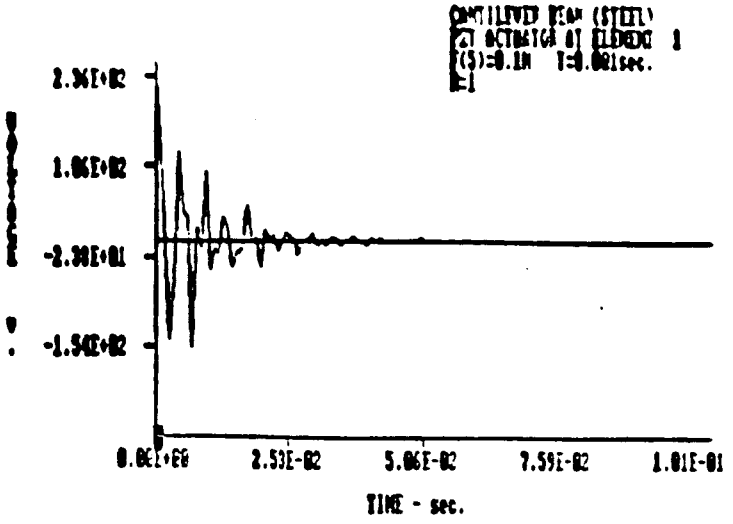

Figure (13-a) - Time history of the control voltages required to control a steel cantilever beam by one PZT actuator placed at element 1 when the weighting factor R=1.

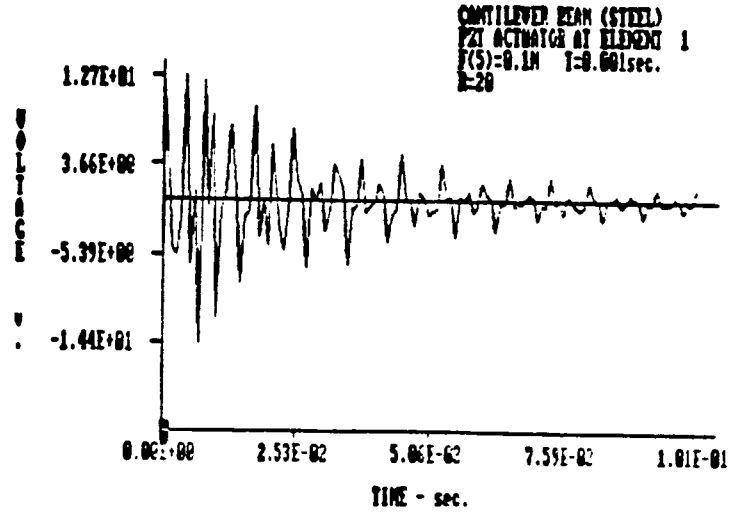

Figure (13-b) - Time history of the control voltages required to control a steel cantilever beam by one PZT actuator placed at element 1 when the weighting factor R=20.

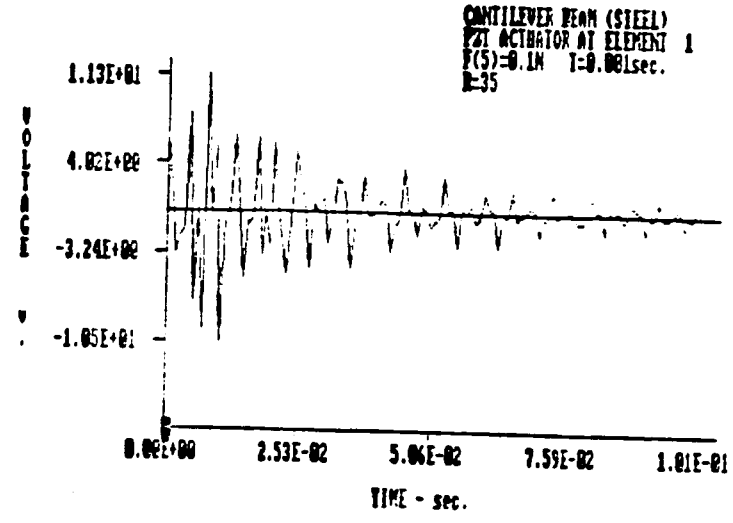

Figure (13-c) - Time history of the control voltages required to control a steel cantilever beam by one PZT actuator placed at element 1 when the weighting factor R=35.

control force and slowing accordingly the process of damping out the structural vibrations. For example, placing equal weigh on the displacement and control force results in maximum amplitude of displacement of 1.26E-5m, as seen from Figure (12-a), but this would require a maximum control voltage of 236v. Increasing the weighting factor R to 35 results in a slight increase in the maximum amplitude of vibration to 1.47E-5m but this is accompanied with a considerable drop in the maximum control voltage to 11.3v as can be seen from Figures (12-c) and (13-c) respectively. According, increasing R, up to 50, results in significant reduction in the control voltage without producing serious degradation in the damping out of the beam vibration. Beyond R=50, it is found that vibration damping process is becoming excessively slow to the extent that overshadows the savings in the control force or the control energy indices.

(ii) Two Actuators

When two PZT piezo-electric actuators are placed at elements 1 and 3 of the steel beam, the resulting time history of the amplitudes of transverse vibrations are shown in Figures (14-a) and (14-b) for values of the weighting factor R of 1 and 20 respectively. Figures (15-a) and (15-b) show the corresponding control voltages.

A summary of the effect of R on the displacement, control force and control energy indices are given in Table

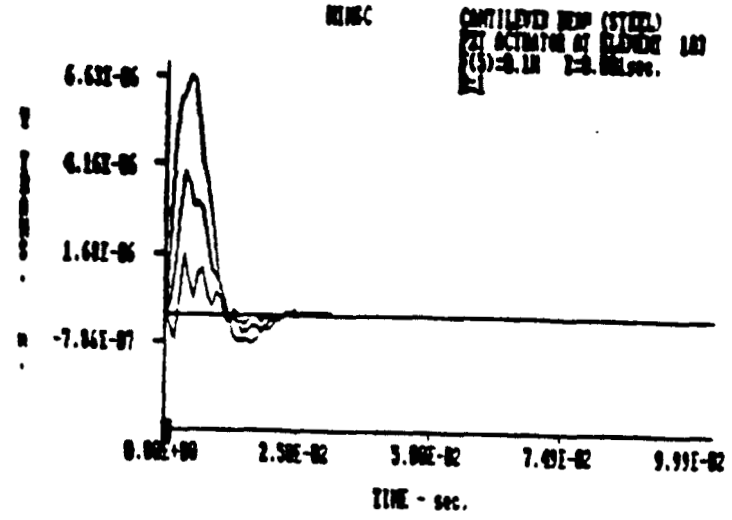

Figure (14-a) - Time history of the amplitudes of transverse vibration of a steel cantilever beam controlled by two PZT actuators placed at elements 1 and 3 when the weighting factor R=1.

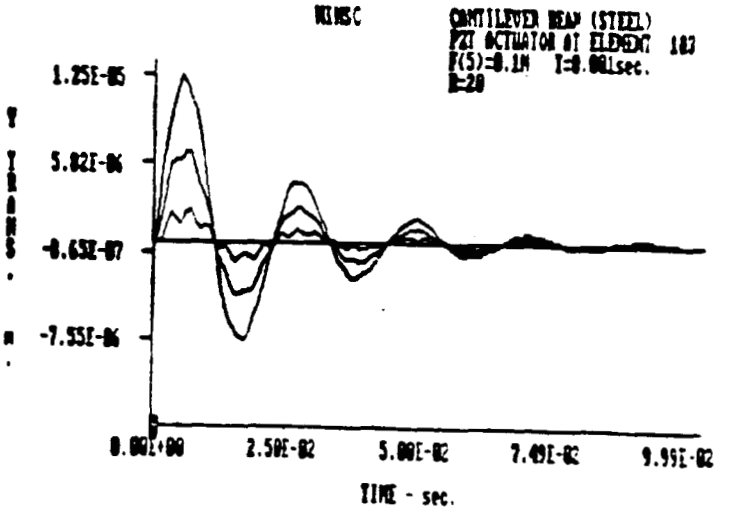

Figure (14-b) - Time history of the amplitudes of transverse vibration of a steel cantilever beam controlled by two PZT actuators placed at elements 1 and 3 when the weighting factor R=20.

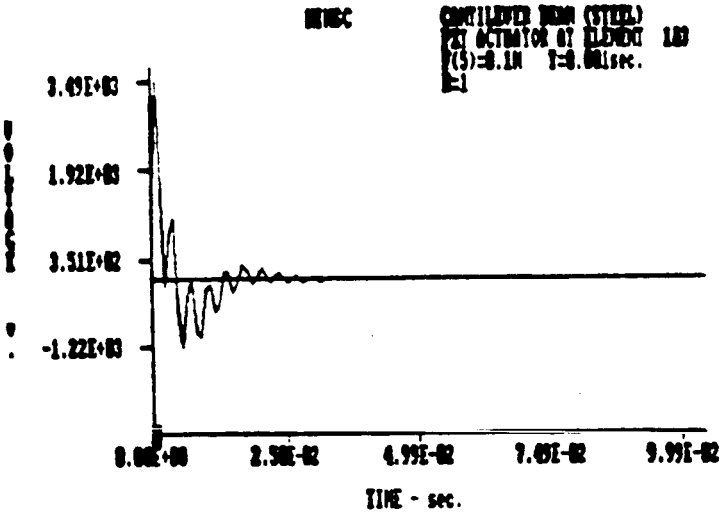

Figure (15-a) - Time history of the control voltages required to control a steel cantilever beam by two PZT actuators placed at elements 1 and 3 when the weighting factor R=1.

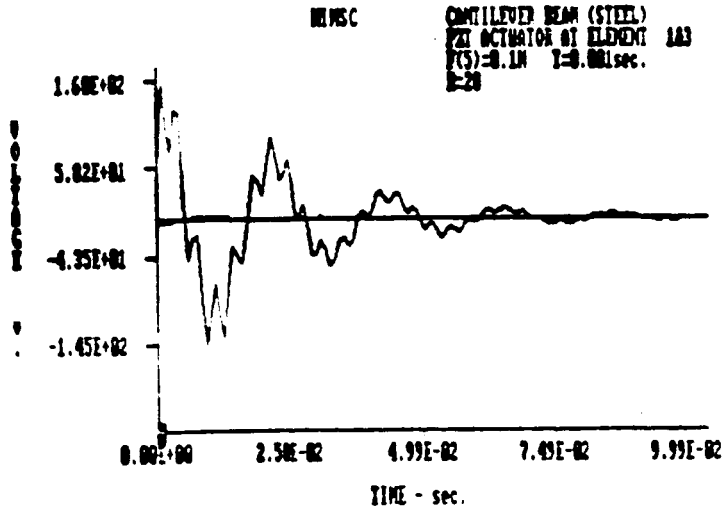

Figure (15-b) - Time history of the control voltages required to control a steel cantilever beam by two PZT actuators placed at elements 1 and 3 when the weighting factor R=20.

(7).

Table (7)- Effect of the weighting factor R on the displacement, control force and control energy indices for a steel cantilever beam controlled by two PZT actuators of thickness=4.2mm placed at elements 1 and 3

Weighting Factor R	1	20	50
Displacement Index, $x10^{9}$	0.0504	0.259	0.4125
Control force Index, $x10^{9}$	23948	119.450	33.2500
Control Energy Index, $x10^{6}$	29.520	2.253	1.4090

Table (7) indicates that increasing R results in reducing the control force and the control energy but at the same time produces higher values of the displacement index. Again, as mentioned before, using two actuators is seen to be more effective in damping out the beam vibrations.

(e) Effect of Beam Material

The effect of changing the material of the cantilever beam, under consideration, from steel to aluminum on the resulting amplitudes of transverse vibrations and the voltage required to control it with one PZT actuator is shown in Figures (16-a) and (16-b) respectively. The actuator has a thickness of 4.2mm and is placed at element 1. The controller is designed with a weighting factor R=50. For this case, the displacement, control force and control energy indices are computed to be 10.4E-9, 19.85E-9 and 0.928E-6 respectively as

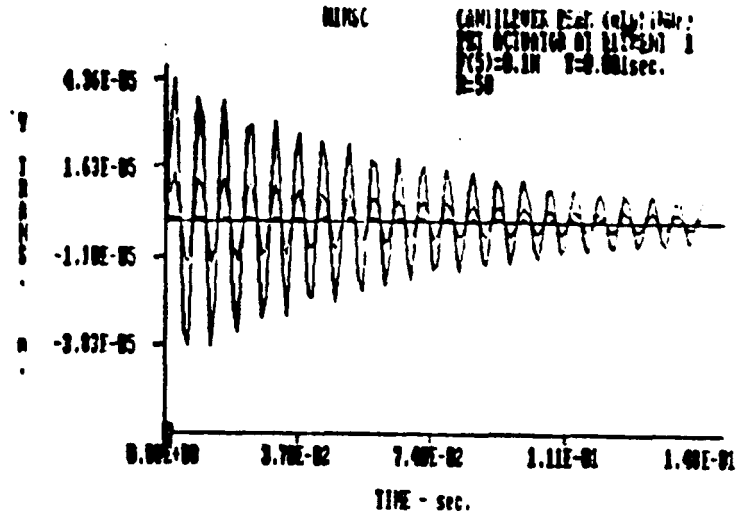

Figure (16-a) - Time history of the amplitudes of transverse vibration of an aluminum cantilever beam controlled by one PZT actuator placed at element 1.

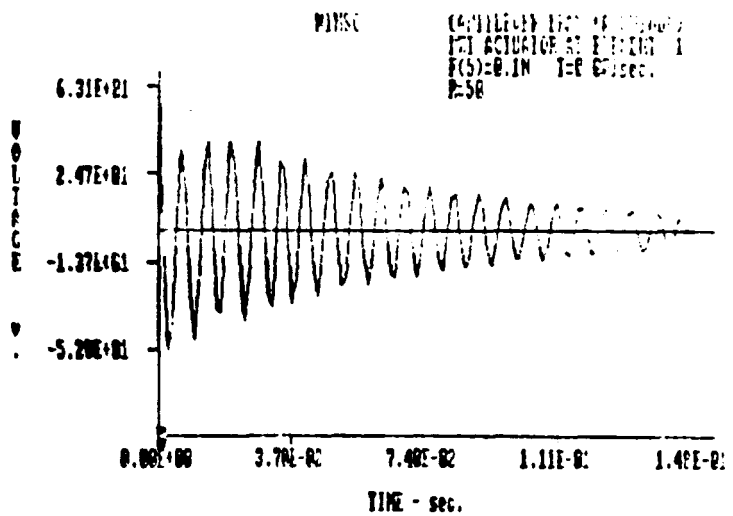

Figure (16-b) - Time history of the control voltages required to control an aluminum cantilever beam by one PZT actuator placed at element 1.

compared to 1.19E-9, 10.34E-9 and 0.307E-6 for the case of the steel beam. Therefore, it is evident that the selected PZT actuator is more effective in damping out the vibration of the steel beam than the aluminum beam.

(f) Effect of Actuator Material

The effect of using a Kynar polymeric actuator, instead of PZT actuator, on the amplitudes of vibration and the voltage required to control the vibration of the aluminum cantilever beam is show in Figures (17-a) and (17-b) respectively. The Kynar actuator is assumed to have a thickness of 4.2mm and be placed at element 1.

A comparison between Figures (16-a) and (17-b) indicates that the maximum amplitude of vibration has increased from 4.36E-5m to 4.88E-5m when the material of the piezo-actuator is changed from PZT to Kynar. This amplitude increase is about 11.9%. But, the required maximum control voltage is found to increase from 63.1 to 141 volts respectively. This amounts to an increase of 123.4%. Therefore, from both the displacement and control voltage, it is preferable for the arrangement under consideration to use PZT actuators.

A detailed analysis of the obtained results indicate that the displacement, control force and control energy indices are 15.28E-9, 5.86E-9 and 0.964E-6 respectively.

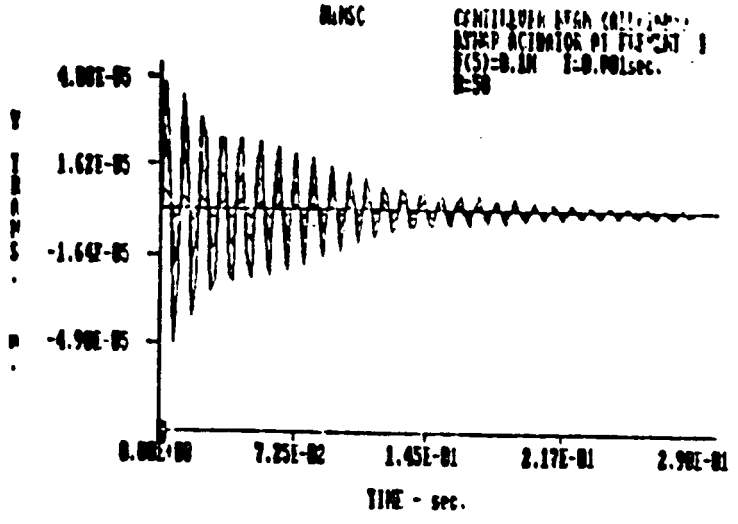

Figure (17-a) - Time history of the amplitudes of transverse vibration of an aluminum cantilever beam controlled by one Kynar actuator placed at element 1.

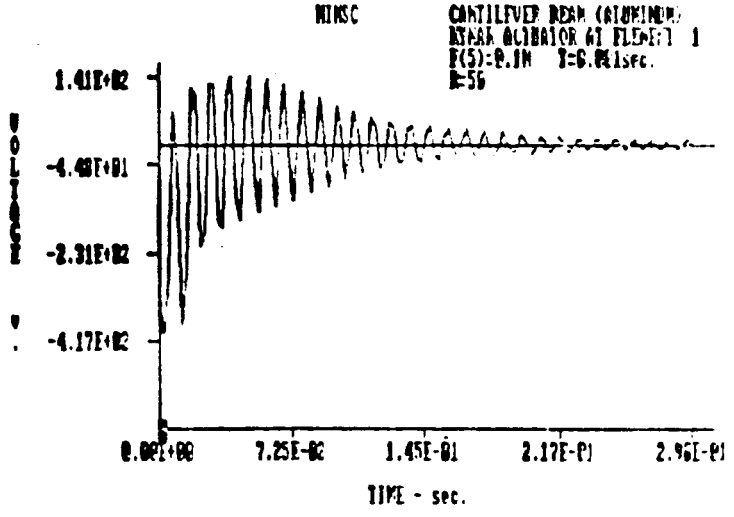

Figure (17-b) - Time history of the control voltages required to control an aluminum cantilever beam by one Kynar actuator placed at element 1.

II. Response to Sinusoidal Loading

The steel cantilever beam, which is controlled by one PZT actuator of thickness 4.2mm placed at element 1, is subjected to external sinusoidal transverse force acting at node 4. The applied force has a magnitude of 0.1N and frequency ranging from 15Hz to 1000Hz.

Figures (18-a), (18-b) and (18-c) show a comparison between the time histories of the amplitudes of vibration of the controlled and uncontrolled beam at frequencies of 100, 900 and 3100 rad/sec respectively.

From these figures, it can be seen that the piezoactuator is capable of attenuating the response of the beam to the sinusoidal excitation throughout the considered range of frequency. The attenuation is however more significant at high frequency than at lower frequencies.

A summary of the effect of the excitation frequency on the ratio of the amplitudes of vibration of the controlled beam to those of the uncontrolled beam, in decibels, is shown in Figure (19). Figure (19-a) displays the linear amplitude ratios and Figure (19-b) shows the angular amplitude ratios for the different nodes.

B. Vibration of Overhung Beam

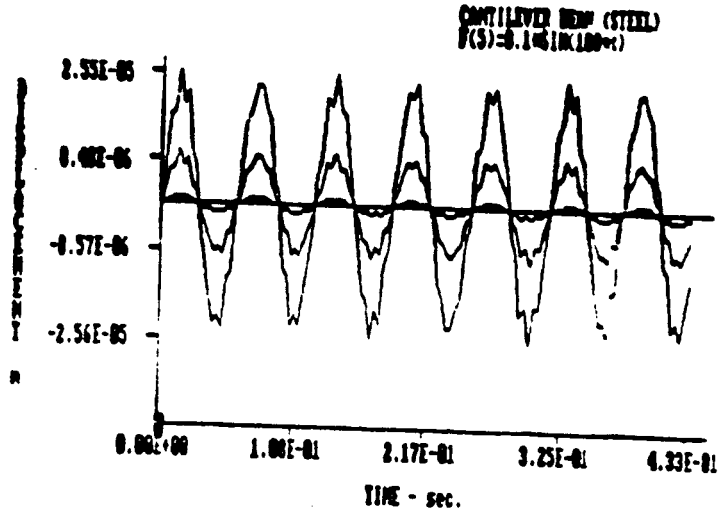

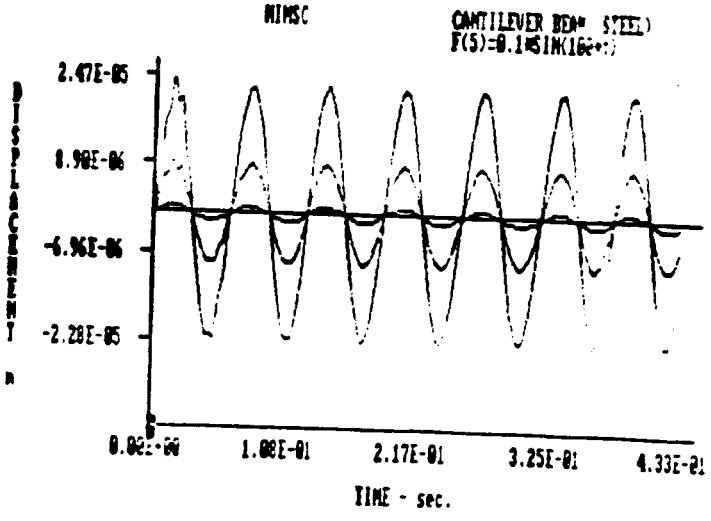

Figure (18-a) - Comparison between the time history of the amplitudes of transverse vibration of uncontrolled and controlled steel cantilever beam when subjected to sinusoidal excitation at frequency = 100 rad/s.

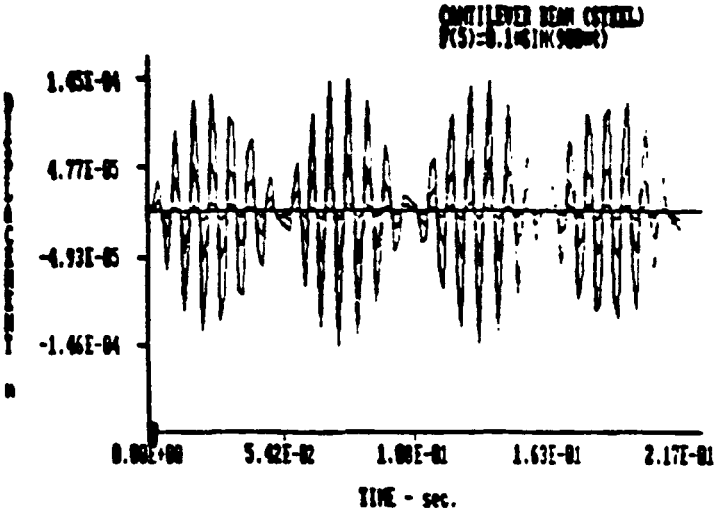

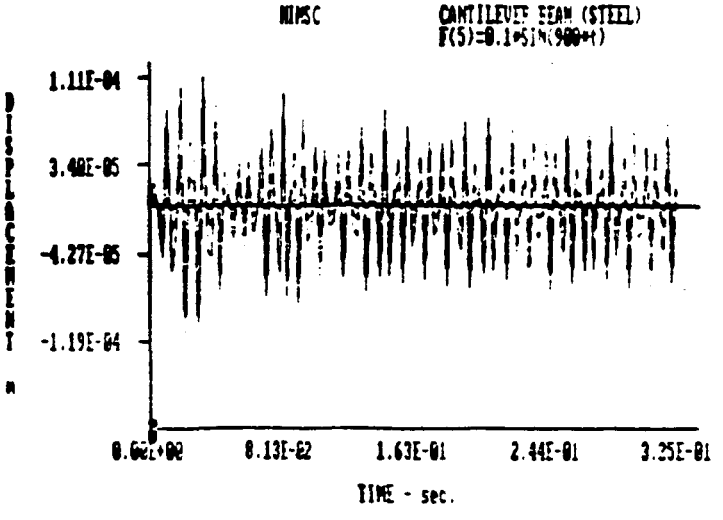

Figure (18-b) - Comparison between the time history of the amplitudes of transverse vibration of uncontrolled and controlled steel cantilever beam when subjected to sinusoidal excitation at frequency = 900 rad/s.

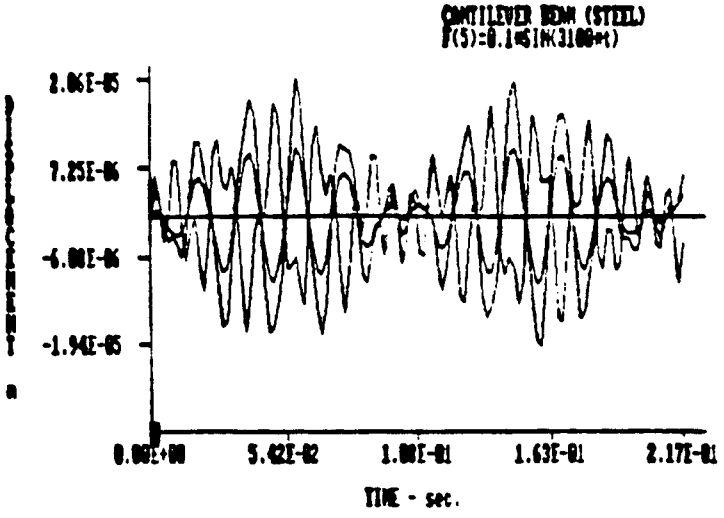

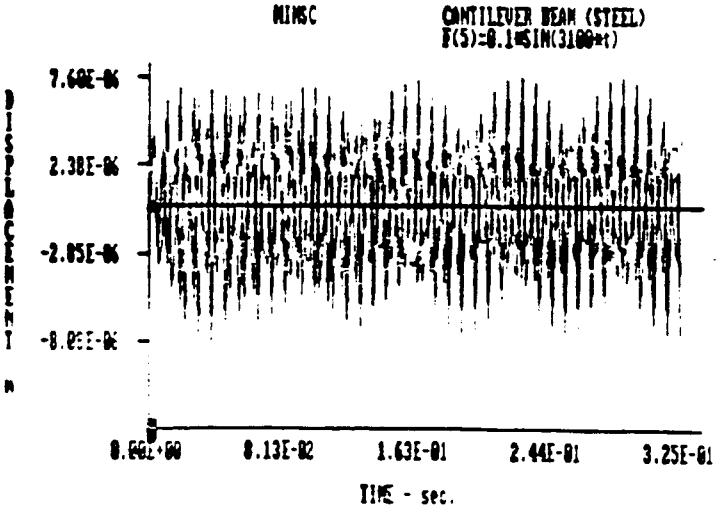

Figure (18-c) - Comparison between the time history of the amplitudes of transverse vibration of uncontrolled and controlled steel cantilever beam when subjected to sinusoidal excitation at frequency = 3100 rad/s.

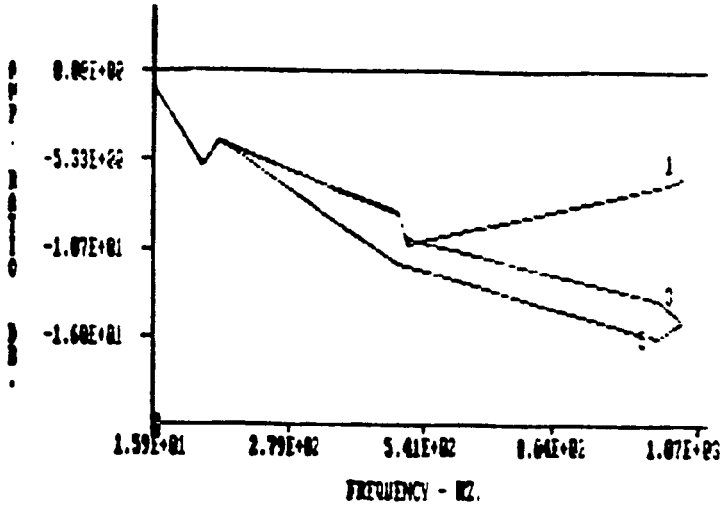

Figure (19-a) - Effect of excitation frequency on the ratio between the amplitudes of linear translation of the uncontrolled and the controlled steel beam.

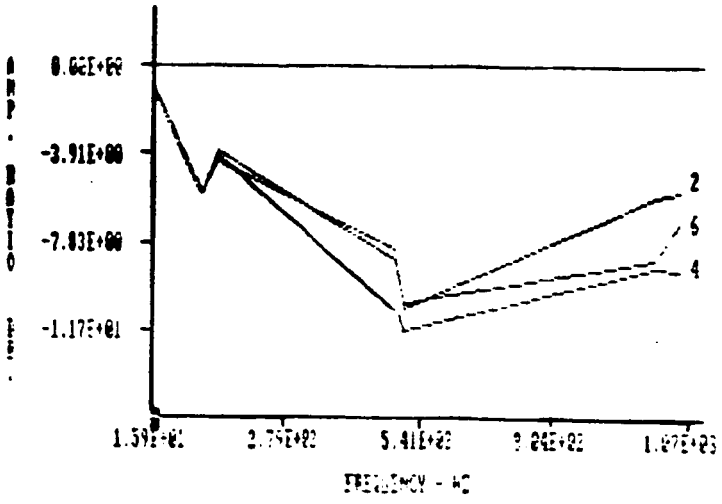

Figure (19-b) - Effect of excitation frequency on the ratio between the amplitudes of angular deflection of the uncontrolled and the controlled steel beam.

The three element steel beam, under consideration, is fixed at node 1 and is restrained from linear transverse motion at node 3. Such configuration is considered as an example to illustrate the effect that the end conditions of a flexible structural element have on its vibration control characteristices.

The effectiveness of the control strategy will be compared to the time history of the amplitudes of vibration of the uncontrolled beam which are shown in Figure (20).

The considered overhung beam is assumed to be controlled by two PZT actuators each has a thickness of 4.2mm. The effect of placing the two actuators at elements 1 and 2, 1 and 3 or 2 and 3 on the time history of the amplitudes of transverse vibration is shown in Figures (21-a), (21-b) and (21-c) respectively when the beam is subjected to an impulse of 0.1N for a duration of 1ms at node 4. The corresponding control voltages are shown in Figures (22-a), (22-b) and (22-c) respectively.

The associated displacement, control force and control energy indices are listed in Table (8).

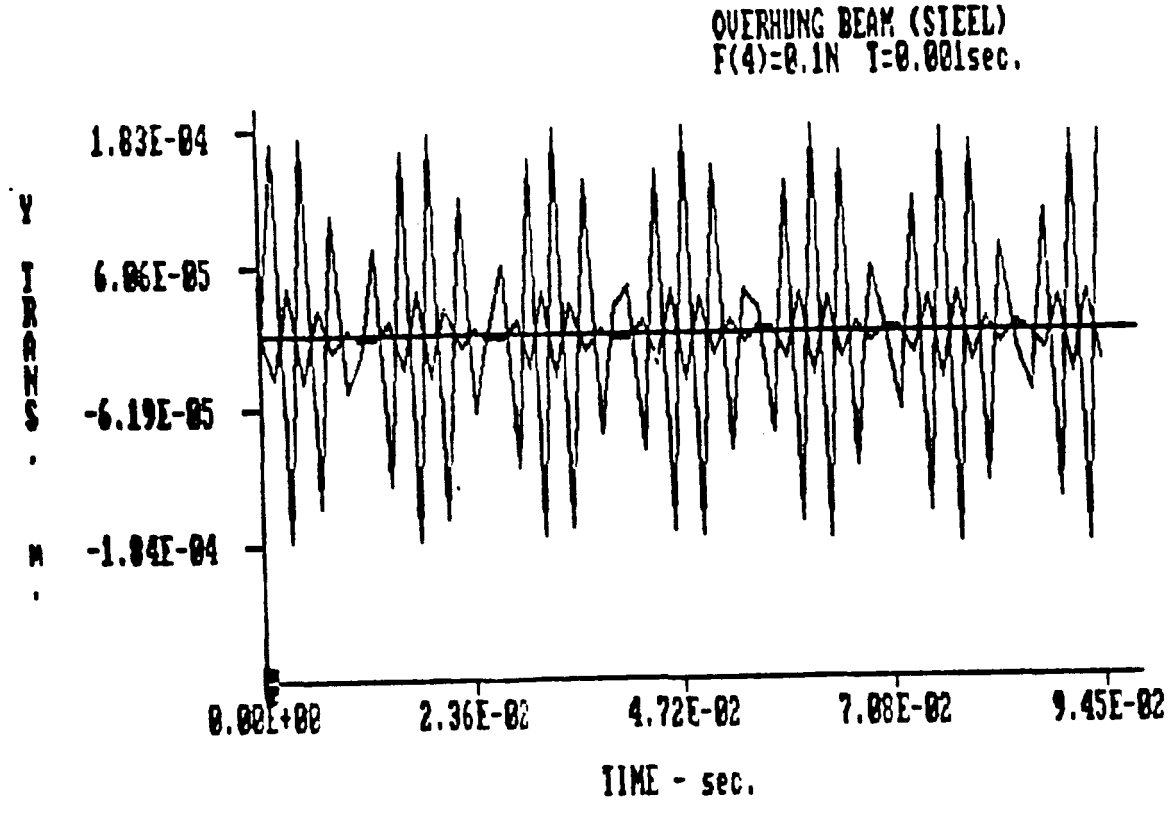

Figure (20) - Time history of the amplitudes of transverse vibration of an uncontrolled overhung steel beam when subjected to transverse impulsive loading.

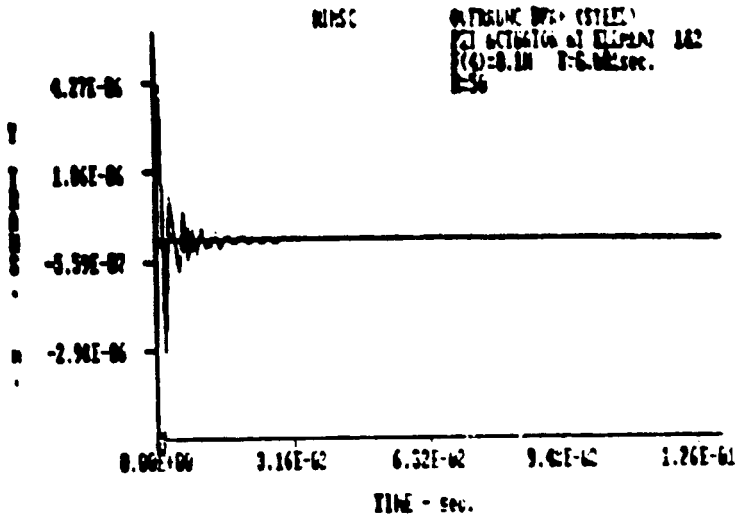

Figure (21-a) - Time history of the amplitudes of transverse vibration of an overhung steel beam when controlled by two PZT actuators of thickness=0.0042 m placed at elements 1 and 2.

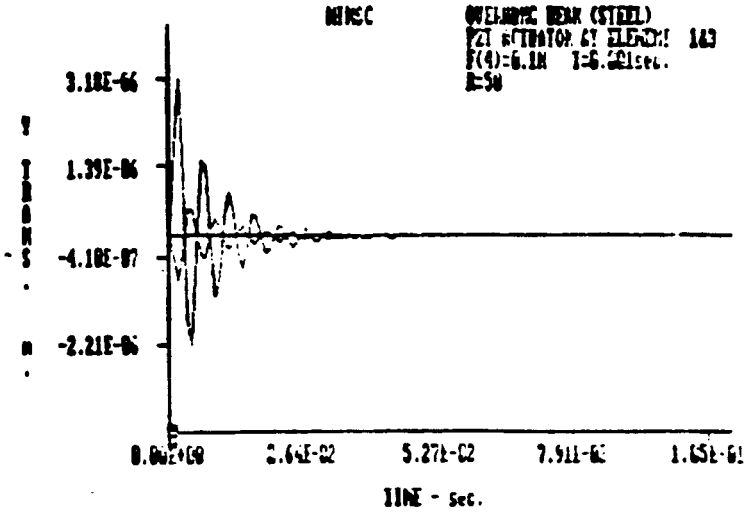

Figure (21-b) - Time history of the amplitudes of transverse vibration of an overhung steel beam when controlled by two PZT actuators of thickness=0.0042 m placed at elements 1 and 3.

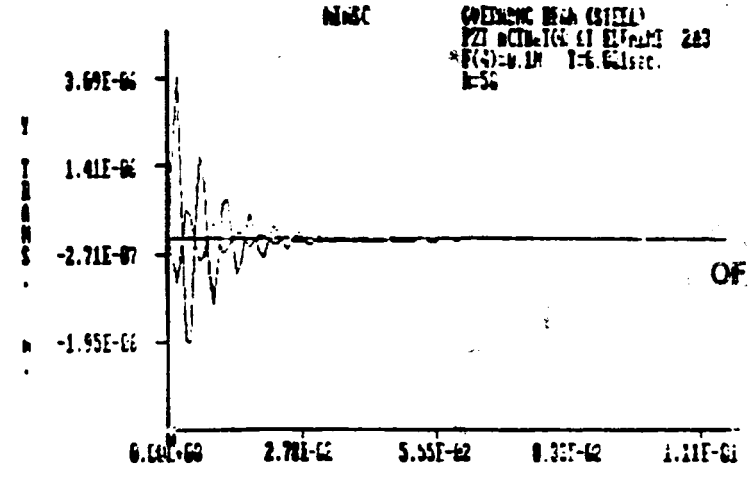

Figure (21-c) - Time history of the amplitudes of transverse vibration of an overhung steel beam when controlled by two PZT actuators of thickness=0.0042 m placed at elements 2 and 3.

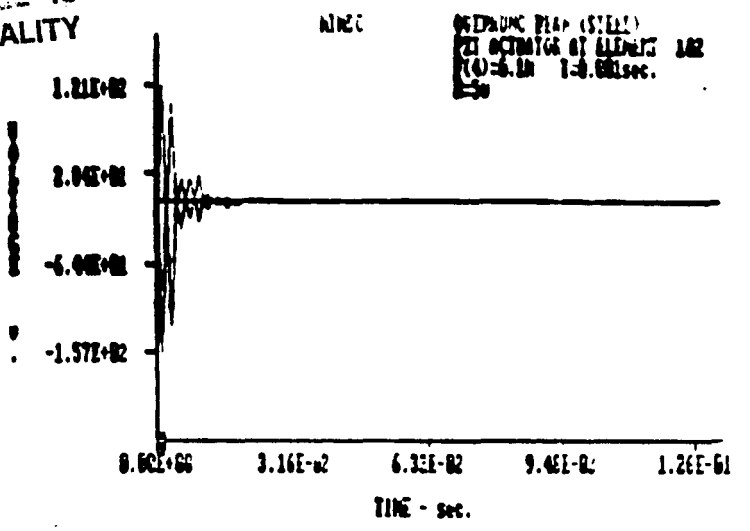

Figure (22-a) - Time history of the control voltages required to control an overhung steel beam by two PZT actuators of thickness=0.0042 m placed at elements 1 and 2.

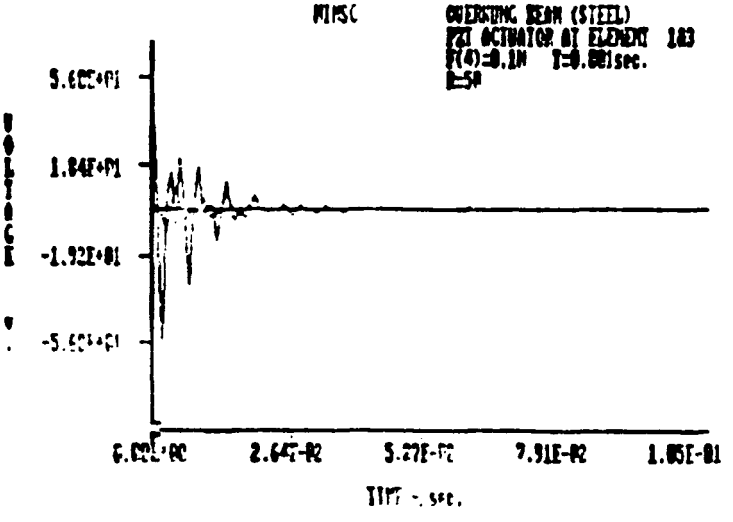

Figure (22-b) - Time history of the control voltages required to control an overhung steel beam by two PZT actuators of thickness=0.0042 m placed at elements 1 and 3.

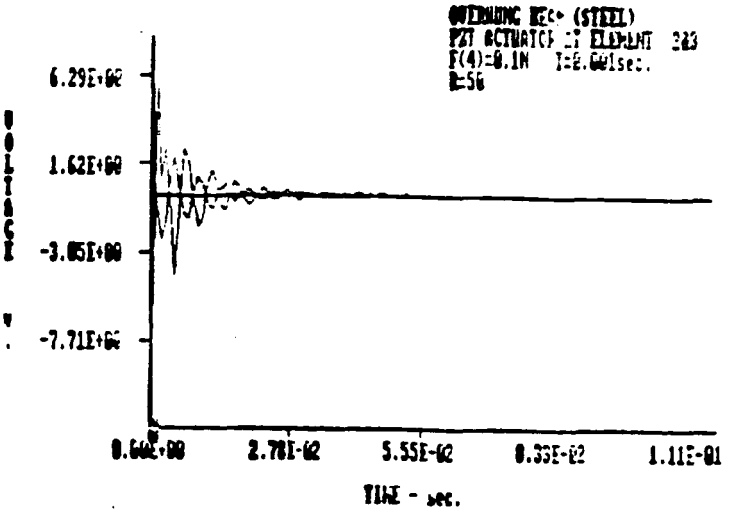

Figure (22-c) - Time history of the control voltages required to control an overhung steel beam by two PZT actuators of thickness=0.0042 m placed at elements 2 and 3.

Table (8) - Effect of placement strategy of two PZT actuators of thickness=4.2mm on the displacement, control force and control energy indices of an overhung steel beam

Actuator Location	Element 1 and 2	Element 1 and 3	Element 2 and 3
Displacement Index, $x10^9$	0.0219	0.0226	0.0221
Control force Index, $x10^9$	7.2520	0.6190	0.1664
Control Energy Index, $x10^6$	9.8900	1.9870	0.9140

The results listed in Table 8 suggest that placing the actuators at elements 2 and 3 results in minimizing the control force and control energy indices simultaneously.

Conclusions

This study has presented a comprehensive analysis of the control of vibration of simple structural elements using piezo-electric actuators. The developed vibration control algorithm is based on a Modified Independent Modal Space Control (MIMSC) method which accounts for the interaction between the controlled and uncontrolled modes, optimal placement of the actuators as well as time sharing of few actuators between the modes of the structure. The method is found to be extremely effective in controlling all the modes of vibration of simple structural elements with very small numbers of actuators.

The MIMSC is developed to account also for the effects that the piezo-electric-based active control system it is essential to determine the optimal actuator geometry, control voltage and location for a particular loading and end conditions. It was concluded that there is an optimal actuator thickness of which the displacement, control force and control energy can be minimized. Thin actuators are ineffective in damping out the vibration whereas thick actuators would require much higher control voltages.

It is observed also that spreading the piezo-electric material over the structural element results in lowering the amplitude of vibration considerably. Furthermore, the study indicated also the importance of selecting the proper

weighting factor between the damping of vibration and the expenditure of control energy.

Using ceramic PZT actuator is seen to be more effective than Kynar actuators in controlling the vibrations of the considered simple structural elements without requiring excessively high control voltages.

The study has demonstrated also the effectiveness of the developed MIMSC method in controlling the vibration of flexible beams made of different materials and subjected to different types of end constraints.

The presented results emphasize the importance of the MIMSC method in designing more realistic active control systems for flexible beam in particular and large flexible structures in general.

The extension of the developed algorithm to large structures can be readily done without any modifications.

REFERENCES

1. Crawley, E.F., and J.de Luis, "Use of piezo-Ceramics as distributed actuators in Large Space Structures", Proc. of the 26th structures, Structure Dynamics and Materials Conference, Part 2, AIAA-ASME-ASCE, Orlando-Florida, pp. 126-133, April 1985.

2. Bailey, T. and James E.Hubbard Jr., "Distributed Piezo-electric Polymer Active Vibration Control of a Cantilever Beam", J. of Guidance and Control, Vol. 8, No. 5, pp. 605-611, Sept.-Oct. 1985.

3. Forward, R.L., "Electronic Damping of Orthogonal Bending Modes in a Cylindrical Mast-Experiment", J. Spacecraft, Vol. 18, No. 1, pp. 11-17, Jan.-Feb. 1981.

4. Lockheed Missiles and Space Company, Inc., "Vibration Control of Space Structures, VCOSS A: High and Low-Authority Hardware Implementations", Report #AFWAL-TR-83-3074, July 1983.

5. Aronson, R.B., (ed.), "Rediscovering Piezoelectrics", Machine Design, Vol. 56, No. 14, pp.73-77, 1984.

6. Toda, M., S. Osaka and E. Johnson, "A new Electromotional Device", RCA Engineer, Vol. 25, No. 1, pp. 24-27, 1979.

7. Toda, M., S. Osaka and S. Tosima, "Large Area Display Element Using PVF2 Bimorph With Double-Support Structure", Ferroelectronics, Vol. 23, pp. 115-120, 1980.

8. Piezo-Electric Products, Inc., "Piezoceramic Design Notes", Sensors, Mar. 1984.

9. Toda, M., "Electromational Device Using PVF2 Multilayer Bimorph", Trans. of the IECE of Japan, vol. E61, No. 7, pp. 507-512, July 1978.

10. Kelly Lee, J. and M. Marcus, "The Deflection-Bandwidth Product of PVF Benders and Related Structures", Ferroelectonics, Vol. 32, pp. 93-101, 1981.

11. Toda, M., "Elastic Properties of Piezo-Electric PVF@", J. Appl. Phys., Vol. 51, No. 9, pp. 4673-4677, Sept. 1980.

12. Baz, A., "Static Deflection Control of Flexible Beams by Piezo-Electric Actuators", NASA Technical Report, Contract No. 30429-D, Sept. 1986.

13. Meirovitch, L. and H. Baruh, "Optimal Control of Damped Flexible Gyroscopic Systems", J. of Guidance and Control,

Vol. 4, No.2, pp. 157-163, 1981.

14. Meirovitch, L. and H. Baruh, "Control of Self-Adjoint Distributed-Parameter Systems", J. of Guidance and Control, Vol. 5, No. 1, pp. 59-66, 1982.

15. Meirovitch, L., H. Baruh and H. Oz, "Comparison of Control Techniques for Large Flexible Systems", J. of Guidance and Control, Vol. 6, No.4, pp. 302-310, 1983.

16. Gere, J.M and S.P. Timoshenko, "Mechanics of Materials", 2nd Edition, Brooks/Cole Engineering Division, Monterey CA, 1984.

17. Paz, M., "Structural Dynamics : Theory and Computation", 2nd Edition, Van Nostrand Reinhold Co, New York, 1985.

18. Bathe, K.J. and E.L. Wilson, "Numerical Methods in Finite Element Analysis", Prentice-Hall Inc., Englewood Cliffs, NJ, 1976.

19. Yang, T. Y., "Finite Element Structural Analysis", Prentice-Hall Inc., Englewood Cliffs, NJ, 1986.

20. Fenner, R.T., "Finite Element Methods for Engineers", McMillan Press Ltd, Londan, 1975.

21. Meirovitch, L., "Analytical Methods in Vibrations", Macmillan Co., NY, 1967.

22. Baz, A. and S. poh, "Modified Independent Modal Space Control Method for Active Control of Flexible Systems", NASA Technical Report, Contract No. 30429-D, Feb. 1987.

23. Reklaitis, G.V., A. Ravindran and K.M. Ragsdell, "Engineering Optimization : Methods and Applications", J. Wiley and Sons, NY, 1983.

24. Pennwalt Corp., "Kynar Piezo-film", King of Prussia, PA, 19406-0018.